Spring 2014

An effectiveness - based analysis of ground coupled heat exchangers

Chou Shen

Department:

AN EFFECTIVENESS - BASED ANALYSIS OF GROUND COUPLED HEAT EXCHANGERS

by

CHOU SHEN

A THESIS

Presented to the Faculty of the Graduate School of the

MISSOURI UNIVERSITY OF SCIENCE AND TECHNOLOGY

In Partial Fulfillment of the Requirements for the Degree

MASTER OF SCIENCE IN MECHANICAL ENGINEERING

2014

Approved by

K. O. Homan, Advisor
A. L. Crosbie
S. W. Baur

ABSTRACT

This thesis develops a theoretical framework, termed $\varepsilon - \mathrm{BLU}$, to characterize the relation between temperatures, thermal contact and borehole length as it relates to the heat transfer processes in ground coupled heat exchangers used for ground source heat pump systems.

Borehole outflow temperature depends on the inflow temperature, the heat imposed on the borehole and the temperature history of the ground. In addition, variation of outflow temperature influences inflow temperature, even for the case of constant heat pump load. Because of this kind of feedback, the borehole inflow temperature may not be constant even with a fixed building load. Considering the complexity, the research is divided into two sections: "open loop" problems and "closed loop"problems. For "open loop" problems, the inflow temperature is specified and taken to be independent of the outflow temperature. The development of the $\varepsilon - \mathrm{BLU}$ analysis begins with the "open loop" problems. The analysis is then extended to "closed loop" problems for which the inflow temperature is dictated by outflow temperature and specified heat pump load. The impact of both steady and periodic loads on the conductance and fluid temperatures are quantified.

In the $\varepsilon - \mathrm{BLU}$ analysis, the dimensionless conductance quantifies time-dependent thermal contact between the circulating fluid and the ground surrounding the borehole. The dimensionless conductance quantifies the quasi-steady heat transfer with only three dimensionless parameters: the Fourier Number, the Biot Number, and the Number of Borehole Length Units. The resulting graphs enable determination of optimal borehole length, a result not previously recognized. Seasonal equivalent conductance and peak borehole outflow temperature are used to evaluate the effect of building loads on heat transfer through the borehole. A multi-year simulation has also been conducted to reveal the behavior of ground heat exchangers under periodic load.

ACKNOWLEDGMENTS

I would like to thank my wife, Jia Zhu, for being such an understanding lady and lovely angel. I know that a lot of this work would not have been possible without her love.

I would like to extend my sincere gratitude and appreciation to my adviser, Dr. K. O. Homan, for his continuous support, leadership, constructive guidance, and friendship. I consider myself very fortunate to have had the opportunity to work with a teacher and friend like Dr. Homan. It was his inspiration, integrity and undying understanding that got many things this far. Especially, I appreciate it so much that he encouraged me to take care of my wife when she was sick and alone. And at the same time, I was given a lot of patience and tolerance when I was late for my research plan. I would say it is not only just a period of study or work in Missouri *S&T*, but also a period of growth in my life.

My sincere appreciation also extends to the members of my committee members, Dr. A. L. Crosbie and Dr. S. W. Baur, for their committed service and support, their ideas, and suggestions that helped improve my work significantly. I have worked with Dr. Baur before I started my thesis. He has been always kind to his colleagues and students. I am very glad to have him be one of my committee members. I have taken a course instructed by Dr. Crosbie. One of the ideas I used to build my model in the thesis comes directly from what I learned from that course. This experience is so meaningful to me.

TABLE OF CONTENTS

Page

LIST OF ILLUSTRATIONS

Figure Page

LIST OF TABLES

LIST OF SYMBOLS

Roman

Bi	Biot Number
BLU	borehole length unit
Fo	Fourier Number
k	conductivity
L	length
$\dot{m}$	mass flow rate
q	heat transfer rate
R	thermal resistance
r	radius
T	temperature
t	time
U	conductance

Greek

α	diffusivity
δ	difference
θ	dimensionless ground temperature

ξ	transformed dimensionless radial coordinate
τ	Fourier-scaled dimensionless time
ϕ	dimensionless fluid temperature

Subscripts

b	borehole
c	cooling
d	design
f	flow
g	ground
h	heating
n	nominal
p	pump
∞	infinite
$*$	dimensionless

1. INTRODUCTION

The design process for ground coupled heat exchangers (GCHEs) utilized in ground source heat pumps (GSHPs) requires consideration of multiple issues. First, the building load varies with time, both daily and seasonally, so the temperature of inlet water into the borehole and the heat flux through the borehole is not constant. Over long time periods, several years or more, the building loads may also change the ground temperature, so as to influence the heat pump performance. Important considerations include configuration of multiple boreholes, individual borehole length and grout thermal properties. The engineering concern is how to determine borehole configurations that provide a balance between performance and cost.

American Society of Heating, Refrigerating and Air-Conditioning Engineer has sponsored a series of research projects to develop design guidelines for GCHEs. In ASHRAE Handbook HVAC Applications [2011], Kavanaugh's approach is adopted as the preferred design method. Kavanaugh's approach focuses on the determination of total required borehole length. To do so, it accounts for three different pulses of heat: long-term heat imbalance, average monthly heat rate during the design month and maximum heat rate for a design day. The method, in effect, estimates unit length thermal resistance which, with required heat duty, enables estimation of total borehole length. Although practical, this approach has its limitations. First, Kavanaugh's approach is based on the cylindrical model with constant heat flux boundary conditions, which is only a rough approximation of the practical situation. Second, the quasi-steady equation is used to calculate only the overall loop length, but fails to determine individual borehole length. Finally, Kavanaugh's approach assumes the heat transfer rate through the borehole is directly propotional to loop length. Our analysis begins from the observation that the fluid temperature varies along the pipe, and since the far field temperature is constant for an isolated borehole, the heat flux

necessarily varies along the length of an individual borehole. This thesis then develops an original approach which incorporates the requirement for a specified temperature change in a borehole passage and its relation to geometry and the time-dependent, fluid-ground thermal conductance.

2. LITERATURE REVIEW

2.1. ANALYTICAL MODELS

A review of the current literature indicates that there are generally two analytical methods used to charactrize the ground heat transfer processes for vertical ground heat exchangers. One is the Kelvin's line source model and the other is the so called cylindrical-source model.

Kelvin's line source model is the basis for the earliest approach to predicting the heat transfer through ground heat exchanger pipes. Ingersoll [1954] cited this model and applied it to calculate the temperature at selected points in the ground. This model assumes the soil to be an infinite medium with uniform properties and initial temperature. The borehole is assumed to be an infinite line source or sink with a constant heat transfer rate which is initiated at time $t = 0$. The heat flow along the length of borehole is neglected. The temperature response of the ground at a specific position is given by,

$$T - T_{g,\infty} = \frac{q'}{2\pi k} I(\eta)$$

where $T_{g,\infty}$ is the initial temperature of the ground, q' is the heat transfer rate per unit length of borehole, and the dimensionless argument to the integral is $\eta = r/(2\sqrt{\alpha t})$, where r is distance from the line source to the point of interest. Note that this can be rewritten as,

$$\frac{q'}{T - T_{g,\infty}} = \frac{2\pi k}{I(\eta)}$$

where the right-hand side may then be recognized as an inverse thermal resistance. The value of the integral term $I(\eta)$ is tabulated by Ingersoll [1954] with respect to values of η. As mentioned above, one of the assumptions made for this model is that the line source

should be infinitely long, so that the heat flux has only a radial component. According to Ingersoll, this equation should be applied only when $\alpha t/r_b^2 > 20$, or else an appreciable error may be produced for a short time or a large pipe diameter. An important extension of Kelvin's line source theory comes from Hart and Couvillion [1986]. The far-field radius is introduced, which is a critical distance to the line source. The far-field radius is given as $4\sqrt{\alpha t}$, depending on the soil thermal diffusivity and the time the line source is active. According to Hart and Couvillion, the temperature of the ground region outside the far-field radius is free from the influence of the line source.

The cylindrical source model, detailed by Carslaw and Jaeger [1947], forms the basis of another widely used approach. With this model, the U-tube pipe is treated as a single pipe centered in the borehole, surrounded by an infinite solid with constant properties. The pipe is assumed to be infinitely long with axial heat transfer neglected.

Assuming a constant heat transfer rate across the borehole boundary beginning at $t = 0$, the analytical solution may be written as [Carslaw and Jaeger, 1947]

$$T - T_{g,\infty} = \frac{q'}{k} G(z, p)$$

where $z \equiv \alpha t/r_b^2$ and $p \equiv r/r_b$. The function $G(z, p)$ depends on time t and distance from the borehole r. Ingersoll [1954] tabulated some values of $G(z, p)$, and Kavanaugh and Rafferty [1997] provided graphical values of $G(z, p)$ when $p = 1$ which represents the surface of the borehole. When $p = 1$, the temperature of the borehole surface is $T(z, 1)$, at a dimensionless time z.

Similarly, the result with a constant surface temperature has also been treated by Carslaw and Jaeger [1947]. In this case the heat transfer rate per unit length is given by

$$q' = k\Delta T F(z)$$

Where ΔT is the temperature difference between the pipe and initial ground temperature. The values of $F(z)$ are tabulated by Ingersoll [1954].

Kavanaugh and Rafferty [1997] has built up a design method for vertical ground coupled heat exchangers, which is based primarily on the cylindrical model with constant heat transfer rate as boundary condition. The unique contribution by Kavanaugh is the method to determine the required total length of pipe loop. The method uses the steady state heat transfer equation, and considers three different pulses of heat, (1) long-term heat imbalance, (2) average monthly heat rate during the design month and (3) maximum heat rate for a short term period during a design day. The primary shortcoming of this approach is the assumption that the heat transfer rate, per unit length, is constant. The temperature variation of the circulated fluid along the borehole length is not accounted for.

Using Kavanaugh's approach, a tabulation or plot of $G(z, p = 1)$ is all that is needed to estimate total borehole length for a specified overall heat load. The ASHRAE Applications Handbook [ASHRAE, 2011] details Kavanaugh's approach as the recommended design method. The limitation however, is that the approach is based on constant heat flux boundary condition, which is far from the true physical condition. Practically, the method suggests the length of an individual borehole will not affect the heat transfer rate, and fails to identify the optional depth for an individual borehole.

2.2. NUMERICAL MODELS

Both the Kelvin line source model and cylindrical source model are one-dimensional analytical results which neglect the axial heat flow along the borehole length. Beginning in the 1980s, several numerical models have been introduced which capture aspects of the multi-dimensional heat transfer.

Eskilson and Claesson [1988] developed a two dimensional model accounting for radial and axial components of heat transfer. It was a breakthrough that both radial and

axial conduction are considered. In addition to that, the model uses finite length borehole and diameter. The fluid borehole thermal resistance is neglected, and the ground temperature response is achieved based on constant boundary temperatures. In addition, Eskilson introduced a superposition technique to simulate the thermal process of a number of thermally interacting boreholes with regard to computation. However, this radial-axial finite difference model is time-consuming, and difficult to be applied in practical ground coupled heat exchanger design process.

Yavuzturk [1999] developed a short time-step model for heat transfer process in vertical heat exchangers. This model uses a series of pie-sectors to approximate the geometry of circular U-tube pipes. A two-dimensional finite volume approach was applied with a several assumptions. First, the three-dimensional effects at the ground surface and the bottom of the U-tube are ignored. The ground is assumed to have uniform thermal properties and finally, the effects of borehole surface temperature change along the depth are only approximated. This model was proposed as a complement to the long time-step model of Eskilson.

In recent years, numerous researchers conducted numerical simulations and validated the models with commercial software or experimental data. Carli and Zarrella [2010] presented a computational capacity resistance model for vertical ground-coupled heat exchangers. This two-dimensional model considered different fluid flow patterns such as a single U-tube, a double U-tube or coaxial pipes. With supply temperature to the heat exchanger, the model can calculate the outflow temperature and the ground temperature distribution. And this model was validated by a commercial software as well as a ground thermal response test and a survey of an office building equipped with a ground coupled heat pump. Su [2011] presented a fast simulation of a vertical U-tube ground heat exchanger using a one-dimensional transient numerical model. This model neglected the vertical variation of temperature of the heat exchanger, and a mesh grid with uniform spatial increment was created. Both heat load and inlet temperature can be used as the input.

This model was compared with analytical models and validated by experimental data of three boreholes. Although each of these studies have considered simulations with different borehole dimensions, the nature of the heat transfer process and its variation along the length of the borehole has not been revealed.

3. AN EFFECTIVENESS-BASED ANALYSIS

The ground source heat pump system with ground coupled heat exchanger can be illustrated as Figure 3.1. In this scheme, the two legs of the U-tube are treated as a single pipe, which is co-axial with the borehole. The borehole is assumed to be immersed in soil which forms an infinite medium having uniform properties and initial temperature. The time-varying building load, $q(t)$, is imposed on the ground heat exchanger. The heat is therefore driven into or absorbed from the ground through the borehole. In this figure, the dimensional fluid temperatures at the inlet and outlet of the borehole are denoted by $T_f(t,0)$ and $T_f(t,L)$, respectively. The far-field ground temperature is $T_{g,\infty}$. Because of the variation in the borehole heat transfer, a variation of $T_f(t,L)$ will influence $T_f(t,0)$ in return. Because of this feedback, the borehole inlet temperature is unlikely to be constant even with a fixed building load. Recognizing the additional complexity associated with this feedback, our analysis is divided into two parts. In the first part, a constant inflow temperature isolates the thermal parameters and borehole geometry from the feedback. In this way, the system behaves like an "open loop". In the second part, the feedback from $T_f(t,L)$ will be added and the influence on the heat transfer performance will be studied. For this part, the system behaves like a "closed loop".

In effect, the "open loop" assumes there is a heat source or heat sink between heat pump and the borehole. The heat source or sink can supply or absorb energy from the circulating fluid, so that the inflow temperature remains constant. Because of the virtual heat source or heat sink, the heat load imposed on the borehole $q_b(t)$ may not be equal to that imposed by the heat pump $q(t)$.

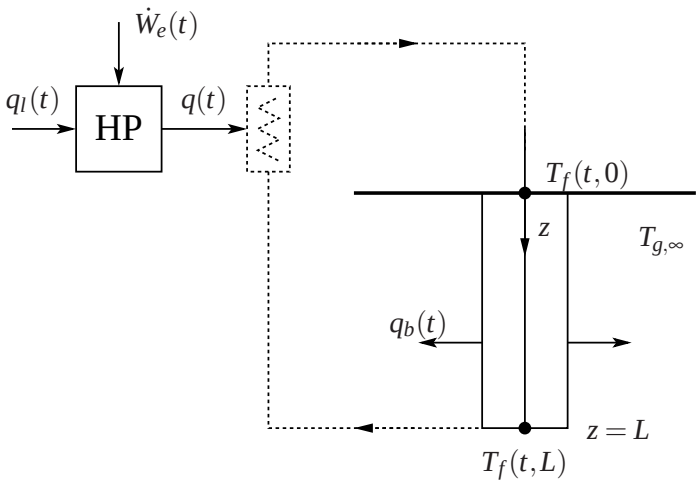

Figure 3.1: The scheme of “open loop”.

3.1. FORMULATION OF EFFECTIVENESS - BLU FRAMEWORK

An energy balance on a differential segment of the borehole yields

$$(\dot{m}C_p)_f \frac{\partial T_f(t,z)}{\partial z} = -U(t,z)P[T_f(t,z) - T_{g,\infty}] \tag{3.1}$$

where $U(t,z)$ is the local conductance between fluid in the borehole and the ground at a far field position, P is the perimeter of borehole surface, and $\dot{m}$ is the mass flow rate of the circulating fluid in the borehole.

The temperature scale is shown in Figure 3.2. The fluid temperature difference from the inlet to the outlet of the heat pump, ΔT_p, is also the temperature difference that, in a real system must be reached across the borehole length. The temperature difference between the borehole inlet and the far field ground temperature is denoted by ΔT_d and defines the temperature limits in the problem. At constant mass flow rate, the cooling and heating loads correspond directly to the temperature differences across the heat pump. The cooling and heating season temperature differences are denoted by $\Delta T_{p,c}$ and $\Delta T_{p,h}$, respectively,

both being positive.

$$q_{p,c} = (\dot{m}C_p)_f \Delta T_{p,c} \tag{3.2}$$

$$q_{p,h} = -(\dot{m}C_p)_f \Delta T_{p,h} \tag{3.3}$$

However, the peak value of the temperature differences driving the fluid-ground heat transfer may be written as

$$\Delta T_{d,c} = T_f(t,0) - T_{g,\infty} = [T_f(t,L) + \Delta T_{p,c}] - T_{g,\infty} \tag{3.4}$$

$$\Delta T_{p,h} = T_{g,\infty} - T_f(t,0) = T_{g,\infty} - [T_f(t,L) - \Delta T_{p,h}] \tag{3.5}$$

The function of the ground heat exchanger is to reverse the temperature change imposed on the circulating fluid by the heat pump, given the fluid-ground temperature difference in the borehole. The ratio of the fluid temperature change to the temperature limits may be recognized as an effectiveness.

$$\varepsilon = \frac{\Delta T_p}{\Delta T_d} \tag{3.6}$$

A dimensionless temperature, depth and time may be defined according to,

$$T^* = \frac{T - T_{g,\infty}}{\Delta T_{d,m}} \tag{3.7}$$

$$z^* = \frac{z}{L} \tag{3.8}$$

$$t^* = \frac{t}{t_s} \tag{3.9}$$

where L represents the borehole length, and t_s denotes one year. The fluid energy balance then becomes,

$$\frac{\partial T_f^*(t^*,z^*)}{\partial z^*} = -\frac{UPL}{(\dot{m}C_p)_f} T_f^*(t^*,z^*) \tag{3.10}$$

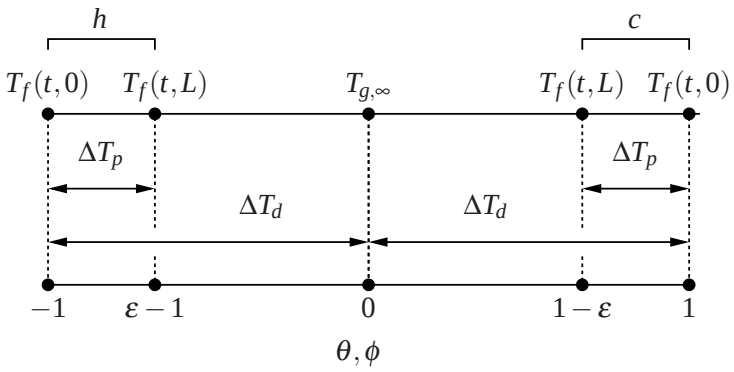

Figure 3.2: The scheme of effectiveness and temperature scale.

Separating the conductance and borehole length into two separate terms:

$$\frac{UPL}{\dot{m}C_p} = \frac{U}{k_g/r_b}\frac{PL}{(\dot{m}C_p)_f} \tag{3.11}$$

two dimensionless parameters can be identified: a dimensionless conductance, $U^*(t^*,z^*)$, and the number of borehole length unit, BLU. The $U^*(t^*,z^*)$ characterizes the thermal contact, which is dependent on time and depth; while the BLU characterizes the borehole geometry, which is independent on time.

$$U^* \equiv \frac{U}{k_g/r_b} \tag{3.12}$$

$$\text{BLU} \equiv \frac{(k_g/r_b)P_bL}{(\dot{m}C_p)_f} \tag{3.13}$$

The fluid energy balance then becomes,

$$\frac{\partial T_f^*(t^*,z^*)}{\partial z^*} = -\text{BLU}\,U^*(t^*,z^*)T_f^*(t^*,z^*) \tag{3.14}$$

defining length average conductance by $\overline{U}^*(t^*) = \int_0^1 U^*(z^*)dz^*$, and integrating Eq. (3.14) over the borehole length, and substituting Eq. (3.6), producing:

$$\varepsilon = 1 - \exp[-\overline{U}^*(t^*)\mathrm{BLU}] \tag{3.15}$$

Equation (3.15) is the basis of the Effectiveness - BLU analysis proposed in this work. The contribution of this equation is that, in a design process, with specified temperature constraints embodied in, ε and dimensionless conductance U^* estimated, the required borehole length unit, BLU, and the required borehole depth can be estimated. The evaluation of the dimensionless conductance is therefore a critically important step. The remainder of this thesis will treat the determination of this dimensionless conductance and its parametric dependence.

3.2. PROBLEM 1: ZERO FLUID-BOREHOLE THERMAL RESISTANCE, INFINITE BOREHOLE LENGTH

The borehole cross section scheme can be illustrated as in Figure 3.3. In this problem, the borehole is assumed to be an infinite long cylindrical heat source, immersed in the soil which is considered as uniform medium of infinite extent. The heat transfer resistance inside the borehole is ignored. The extent temperature along the cylindrical surface is uniform and there is no axial heat transfer along the borehole depth. The dimensional temperature distribution in the ground can be described as Eq. (3.16).

$$\frac{\partial T}{\partial t} = \frac{\alpha}{r}\frac{\partial}{\partial r}(r\frac{\partial T}{\partial r}) \tag{3.16}$$

Taking dimensionless radius as

$$r^* = \frac{r}{r_b} \tag{3.17}$$

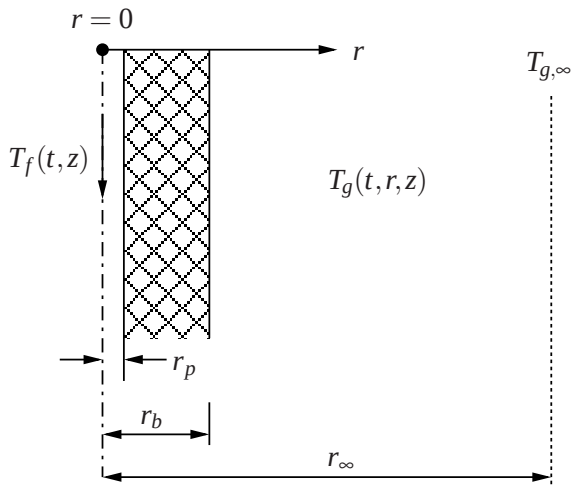

Figure 3.3: The borehole cross section scheme.

where r_b is the borehole radius, and substituting this definition and that of the dimensionless temperature,

$$\frac{\partial T^*}{\partial(\alpha t/r_b^2)} = \frac{1}{r^*}\frac{\partial}{\partial r^*}(r^*\frac{\partial T^*}{\partial r^*}) \tag{3.18}$$

where group $\alpha t/r_b^2$ may be identified as the "time-to-pipe" ratio was firstly introduced by Carslaw and Jaeger [1947]. This parameter represents dimensionless time as measured relative to a ground diffusivity time scale. In ASHRAE terminlogy, this parameter is referred as Fourier number, Fo. According to the definition, different combinations of ground conductivity and time may produce the same value of Fo. Recognizing that there is an essential additional time scale, the time associated with the seasonal load variation, diffusion is not elected as the time scale. The time scale for seasonal variation, t_s, is one year. As a result, this dimensionless parameter is determined only by ground diffusivity and borehole radius. For the computation in this study, a default value of Fo is selected as 10^4. Substitute this definition of Fo.

$$\frac{\partial T^*}{\partial(t^*\mathrm{Fo})} = \frac{1}{r^*}\frac{\partial}{\partial r^*}(r^*\frac{\partial T^*}{\partial r^*}) \tag{3.19}$$

The dimensionless ground temperature $T^*(t^*, r^*)$ is therefore a function of dimensionless time t^* and distance r^*, so the temperature contour will be a series of concentric circles. Since these circles should be denser in the neighborhood of the borehole surface than in the far field, a grid clustering transformation is introduced to resolve the sharp gradients at $r^* \cong 1$.

$$r^* = (\frac{r_\infty}{r_b})^\xi = r_\infty^{*\,\xi} \tag{3.20}$$

The far field radius is denoted by r_∞ and represents the radius at which ground temperature is unaffected by heat flow from the borehole. This is, in effect, a computational boundary. This transformation maps r to ξ, where $\xi = 0$ is associated with $r^* = 1$, and the position where $\xi = 1$ is associated with $r^* = r_\infty^*$.

Substituting Eq. (3.20) into Eq. (3.19), the partial differential equation (PDE) for dimensionless temperature can be written as,

$$\frac{\partial \theta}{\partial \tau} = \frac{1}{(\ln r_\infty^*)^2} \frac{1}{(r_\infty^*)^{2\xi}} \frac{\partial^2 \theta}{\partial \xi^2} \tag{3.21}$$

The dimensionless temperature, $\theta(\tau, \xi)$ is defined by,

$$\theta(t^* \mathrm{Fo}, \ln r^* / \ln r_\infty^*) = T^*(t^*, r^*; \mathrm{Fo}, r_\infty^*)$$

where $\tau \equiv t^* \mathrm{Fo}$, and represents a Fourier-scaled dimensionless time. Since this is a one dimensional diffusion equation, a simple implicit scheme is applied to solve the PDE,

$$\frac{1}{\Delta\tau}(\theta_i^{n+1} - \theta_i^n) = \frac{1}{(\ln r_\infty^*)^2} \frac{1}{(r_\infty^*)^{2i\Delta\xi}} \frac{1}{\Delta\xi^2}(\theta_{i+1}^{n+1} + \theta_{i-1}^{n+1} - 2\theta_i^{n+1}) \tag{3.22}$$

where subscript i denotes space dimension and superscript n notates time, $\Delta\tau$ is dimensionless time step and $\Delta\xi$ is dimensionless spatial grid size. Although the simple implicit scheme is unconditionally stable, $\Delta\tau$ is selected to satisfy explicit stability to produce good

accuracy. The far field radius $r^*_\infty = r_\infty/r_b$ is a constant, and was selected large enough to have no impact on the solution. A value of 100 has been selected. Several cases were run to verify that $r^*_\infty = 100$ was sufficiently large. A spatial increment, in computational coordinates, of $\Delta\xi = 0.001$ is used in computation.

Recalling the definition of t^*, the dimensionless time t^* varies from 0 to 1 over one year. The dimensionless time step $\Delta t^* = \Delta\tau/\mathrm{Fo} = 0.02/\mathrm{Fo}$, which is associated with a period of physical time varying from 0.5 to 5 minutes for typical values of Fo. ASHRAE [2011] suggests values for some thermal parameters and geometries, which are quoted in Table 3.1. Based on these parameters, several dimensionless parameters can be determined, shown in Table 3.2.

As a starting point, $U(t)$ is determined by taking the fluid temperature constant,

$$\phi(\tau, 0) = 1 \tag{3.23}$$

where ϕ represents the dimensionless fluid temperature,

$$\phi(t^*\mathrm{Fo}, z^* = 0) = T^*_f(t^*, z^* = 0; \mathrm{Fo})$$

The initial ground temperature is uniform,

$$\theta(0, \xi) = 0 \tag{3.24}$$

and ignoring the resistance from fluid to borehole surface,

$$\theta(\tau, \xi = 0) = 1 \tag{3.25}$$

The dimensional conductance U is defined by:

$$U = \frac{q_b''}{T_f - T_{g,\infty}} \tag{3.26}$$

where q_b'' is the heat flux through the borehole surface. Applying Fourier's law,

$$U = -\frac{k_g}{T_f - T_{g,\infty}} \frac{\partial T}{\partial r}\bigg|_{r=r_b} \tag{3.27}$$

Substituting Eq. (3.12) into Eq. (3.27)

$$U^*(t^*) = -\frac{1}{T_f^*} \frac{\partial T^*}{\partial r^*}\bigg|_{r^*=1} \tag{3.28}$$

and in computational coordinates

$$U^*(\tau) = -\frac{1}{\phi} \frac{1}{\ln r_\infty^*} \frac{\partial \theta}{\partial \xi}\bigg|_{\xi=0} \tag{3.29}$$

In this way, the dimensionless conductance U^* can be determined by solving Eq. (3.21). The analytical solution for this problem is given by Carslaw and Jaeger in terms of heat transfer rate per unit length,

$$q_b' = k_g(T_f - T_{g,\infty})F(\tau)$$

where as before, $\tau = t^*\mathrm{Fo} = \alpha t / r_b^2$. Substituting this equation into the definition of dimensionless conductance, $U^* = F(\tau)/2\pi$. This analytical result is an important verification of the accuracy obtained by numerical method, and represents a simplest analytical model for the time-dependent conductance associated with the ground heat transfer.

The numerical results for dimensionless conductance U_g^* is shown in Figure 3.4, for dimensionless time t^* from 0 to 1, a physical period of one year. The subscript g is added to the numerically-computed conductance to highlight the fact that the sole contribution to

Table 3.1: Typical range of dimensional properties and geometries.

Properties	Units	Minimum	Maximum
α	m^2/day	0.042	0.14
r_b	mm	50	75
r_p	mm	10	20
k_g	w/mk	0.5	3.8
k_b	w/mk	0.7	2.4
h	w/m^2k	50	2.100
L	m	15	350
$\dot{m}$	kg/m	0.5	20
$T_{g\infty}$	$^\circ F$	45	70
$T_{fc}(t,0)$	$^\circ F$	85	95
$T_{fh}(t,0)$	$^\circ F$	60	80
ΔT_p	$^\circ F$	10	35
ΔT_{dc}	$^\circ F$	20	30
ΔT_{dh}	$^\circ F$	10	20

Table 3.2: Typical range of dimensionless parameters.

Parameters	Minimum	Maximum
Fo	2000	20000
Bi	0.05	5
ε	0.15	0.9
BLU	0.05	200

the conductance is the ground. The numerical results match well with the analytical results provided by Ingersoll. The total conductance decreases rapidly and then more slowly, as time advances. The dimensionless conductance finally reaches a nominally steady value at approximately $t^* = 0.2$. Any time variation of conductance is barely detectable at one year.

To further characterize the transient behavior of dimensionless conductance, three distinct periods are identified. They are the startup period, the transition period and the stable period. The three periods are separated by two defined times. The time separating the startup period and transition period is referred to as transition time t^*_{tr}, and the instant

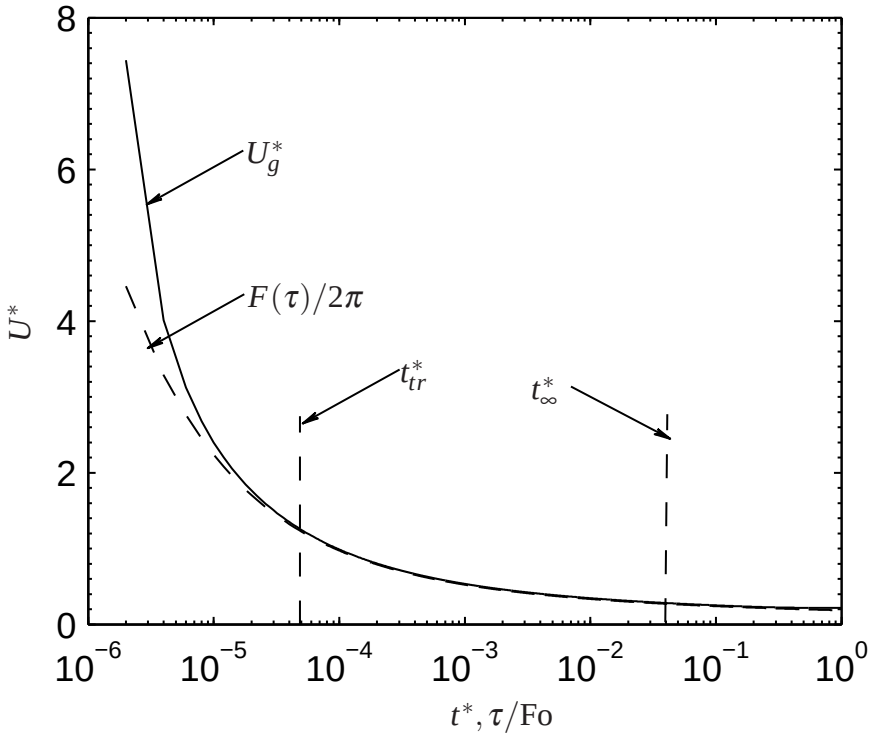

Figure 3.4: Comparison of numerical results U_g^* from Problem 1 and analytical result by Ingersoll [1954].

separating the transition period and stable period is called t_∞^*. These two dividing times are defined by Eq. (3.30) and Eq. (3.31).

$$\left|\frac{dU^*}{d(t^*\mathrm{Fo})}\right|_{t^*=t_{tr}^*} = 1 \tag{3.30}$$

$$\left|\frac{dU^*}{d(t^*\mathrm{Fo})}\right|_{t^*=t_\infty^*} = 10^{-4} \tag{3.31}$$

For Problem 1, with a nominal value of $\mathrm{Fo} = 10^4$, the values of t_{tr}^* and t_∞^* are 4.6×10^{-5} and 3.83×10^{-2}, respectively, which correspond to 0.4 hour and 4 days, respectively. The values of the dimensional conductance at these times are $U^*(t_{tr}^*) = 1.2836$ and $U^*(t_\infty^*) = 0.2837$.

3.3. PROBLEM 2: FINITE FLUID-BOREHOLE THERMAL RESISTANCE, INFINITE BOREHOLE LENGTH

Identifying R_b as the thermal resistance of the borehole, inclusive of the convective resistance, which is associated with fluid flowing through the pipe, and the conductive resistance of the borehole material, it appears in series to the thermal resistance of the ground, R_g. The rate of heat transfer from fluid to borehole surface may then be written as,

$$q'_b(t) = \frac{1}{R'_b}[T_f(t) - T(t, r_b)], \tag{3.32}$$

and invoking Fourier's law,

$$\frac{1}{R'_b}[T_f(t) - T(t, r_b)] = -k_g 2\pi r_b \frac{\partial T}{\partial r}\bigg|_{r=r_b} \tag{3.33}$$

rewriting in dimensionless form,

$$\frac{1}{\ln r^*_\infty}\frac{\partial \theta}{\partial \xi}\bigg|_{\xi=0} = -\frac{1}{2\pi k_g R'_b}[\phi(\tau) - \theta(\tau, 0)] \tag{3.34}$$

This statement provides a Robin type boundary condition for the diffusion equation. Problem 2 may therefore be summarized by Eq. (3.34), Eq. (3.21) and following boundary conditions:

$$\phi(\tau) = 1$$

$$\theta(0, \xi) = 0$$

In Eq. (3.34), the dimensionless quantity $1/(2\pi k_g R'_b)$ represents the ratio of ground conduction resistance and convection resistance in the borehole. This term therefore plays a role similar to a Biot Number, which is an index of the ratio of the conduction resistances inside a body and convection resistance at the surface [Incropera, 2007]. Therefore the Biot

Number can be defined,

$$Bi \equiv \frac{1}{2\pi k_g R'_b} \tag{3.35}$$

and substitute this definition into Eq. (3.29)

$$U^*(\tau) = \mathrm{Bi}[\phi(\tau) - \theta(\tau, 0)] \tag{3.36}$$

It can be observed from Eq. (3.36), conductance U^* is dependent on time t^*, and parametrically on Fo and Bi. The Biot Number, Bi is determined completely by borehole resistance R'_b and ground conductivity k_g. As the borehole resistance goes to zero, Bi grows large, and can be ignored. In that limit, the Problem 2 results will approach those of Problem 1.

Figure 3.5 indicates how U^* varies with t^* at several Biot Numbers, Bi. It can be observed that for Problem 2, when Bi is small, the U^* is very small and doesn't change significantly with time; when Bi increases, U^* tends to behave in the same pattern as that of Problem 1. These observations are clearly in agreement with the discussion above.

How Bi will influence U^* can be seen more clearly if the conductance U^* and Bi are scaled by dimensionless conductance as determined by Problem 1. Figure 3.6 shows how U^*/U_g^* varies with Bi/U_g^*. The dimensionless conductance, U_g^*, represents dimensionless conductance associated with the ground alone, from Problem 1. This scaling clearly eliminates the time dependence of U^*. It can be observed from this figure that the influence of borehole resistance won't be amplified when time increases. In a word, Bi dominates heat transfer when it is relatively small, however when it is larger than $\mathrm{Bi}/U_g^* \simeq 10$, the borehole resistance can be ignored. Dimensionless conductance can be read from this figure and there is no need to compute cases with different Bi. This observation is very useful for choosing suitable material used in the borehole.

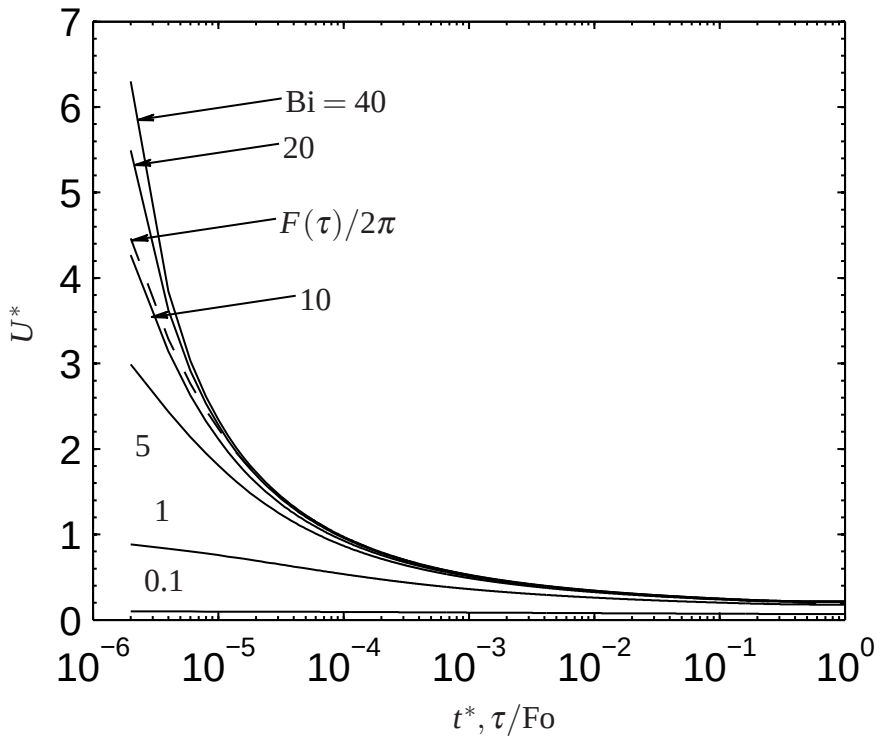

Figure 3.5: Comparison of U^* with different Bi from Problem 2 and analytical result by Ingersoll [1954].

3.4. PROBLEM 3: ZERO FLUID-BOREHOLE THERMAL RESISTANCE, FINITE BOREHOLE LENGTH

The fluid temperature in the borehole varies with depth, so the ground temperature must vary not only in the radial direction, but also in the depth direction. The previous two problems have, however, ignored this reality. As a first approximation the vertical heat conduction in the ground is negligible compared with radial conduction; while the boundary condition, based on fluid temperature, is different along depth. In this way, the problem is transferred to a series of problems similar to Problem 1, with varying fluid temperature forming a Dirichlet boundary condition. In dimensionless form, the fluid energy balance,

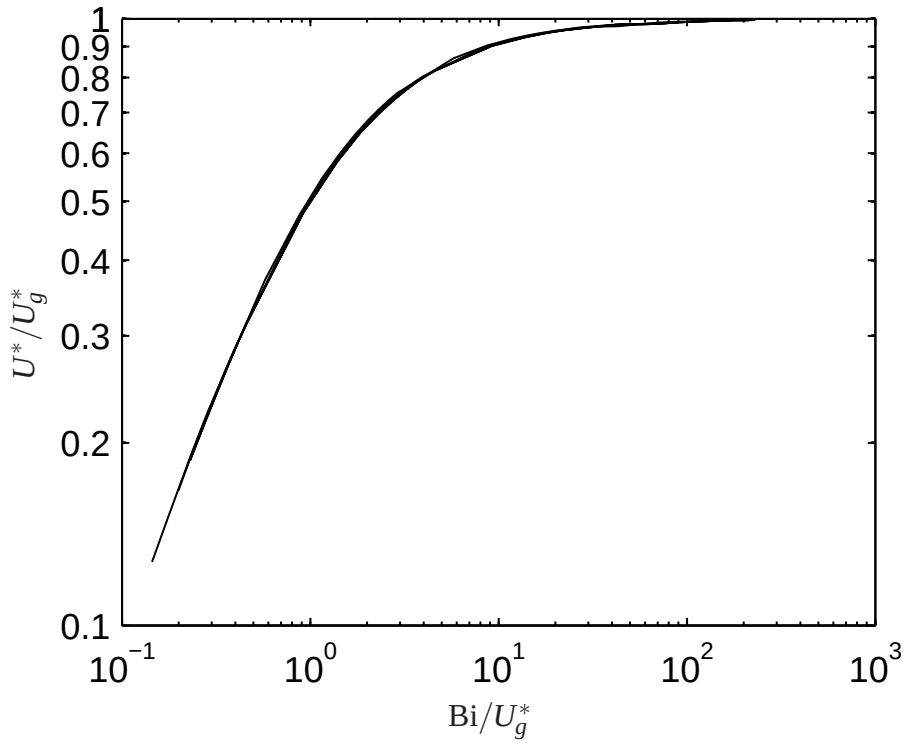

Figure 3.6: U^*/U_g^* with respect to Bi/U_g^* at different time t^*. In this figure, the results are shown in the situations when dimensionless time $t^* = 0.01$, $t^* = 0.1$, $t^* = 1$, $t^* = 5$, $t^* = 10$ and $t^* = 20$. The difference between these results are clearly indistinguishable.

Eq. (3.14), is then,

$$\frac{\partial \phi(\tau, z^*)}{\partial z^*} = -U^*(\tau, z^*)\phi(\tau, z^*)\mathrm{BLU} \tag{3.37}$$

With the boundary conditions as follow, Eq. (3.37) and Eq. (3.21) can be used to compute $\phi(\tau, z^*)$ and $\theta(\tau, z^*, \xi)$. Figure 3.7 shows how the dimensionless conductance $U^*(\tau, z^*)$ varies along borehole depth.

$$\phi(\tau, 0) = 1 \tag{3.38}$$

$$\theta(0, z^*, \xi) = 0 \tag{3.39}$$

$$\phi(\tau, z^*) = \theta(\tau, z^*, 0) \tag{3.40}$$

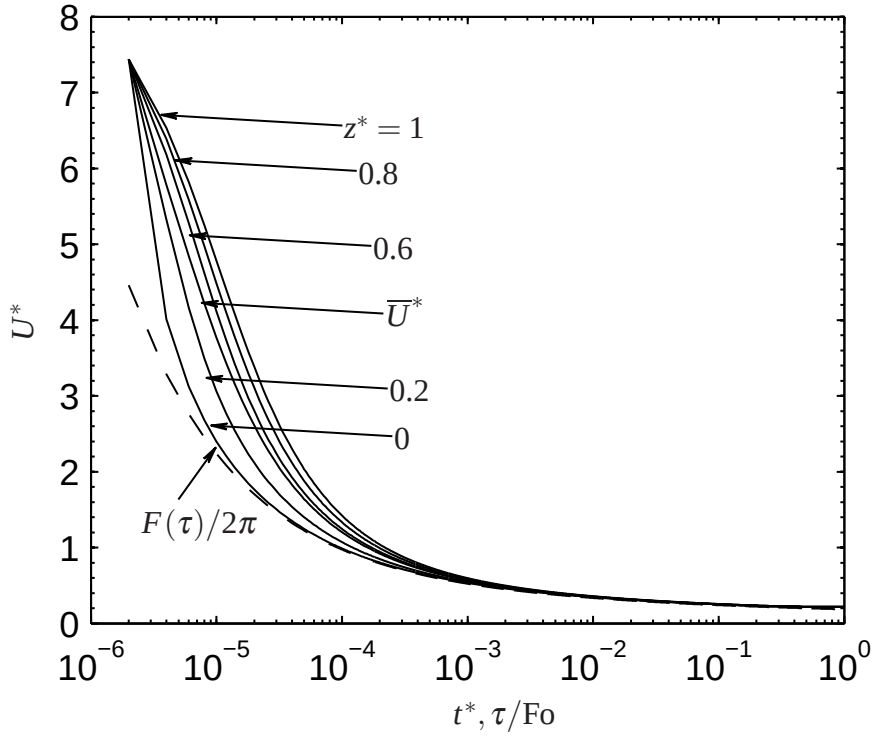

Figure 3.7: Comparison of U^* at different depth z^* for Problem 3 and analytical results by Ingersoll [1954], with BLU $= 1.5$.

The conductance behaves in a similar pattern at different depth. The finite borehole length effect does enhance the heat transfer compared to Problem 1, since the conductance increases along the borehole depth, particularly in the initial period. At larger times when the conductance decreases slowly, the conductance variation along the depth is indistinguishable. As a result, a conservative approach to estimating U^* would be using the conductance without considering the influence from borehole length.

Before further analysis, an important concept, dimensionless break through time, t_b^*, is introduced. The heat transfer rate over the borehole can be expressed as:

$$q_b = (\dot{m}C_p)_f [T_f(t,0) - T_f(t,L)] \tag{3.41}$$

The dimensionless borehole load is then

$$q_b^*(t^*) = \frac{q_b}{(\dot{m}C_p)_f \Delta T_p} \tag{3.42}$$

Substituting Eq. (3.41) and Eq. (3.6) into Eq. (3.42) produces,

$$T_f^*(t^*,0) = T_f^*(t^*,1) + \varepsilon q_b^*(t^*) \tag{3.43}$$

In terms of θ and ϕ,

$$q_b^*(\tau) = \frac{1}{\varepsilon}[\phi(\tau,0) - \phi(\tau,1)] \tag{3.44}$$

Under quasi-steady conditions, the heat transfer rate imposed by the heat pump should be equal to the heat transfer rate over the borehole length, so $q_b^* = q^*$. But for the "open loop" problem, this relationship may not exist, because inlet temperature is specified and, in effect, there must be a heat sink or source between the heat pump and borehole to satisfy the fixed inlet temperature condition.

Defining length average conductance $\overline{U}^*(\tau)$, and integrating Eq. (3.37) over the borehole length,

$$\phi(\tau,1) = \phi(\tau,0)\exp[-\overline{U}^*(\tau)\mathrm{BLU}] \tag{3.45}$$

substitute Eq. (3.45) into Eq. (3.44)

$$q_b^*(\tau) = \frac{\phi(\tau,0)}{\varepsilon}\{1 - \exp[-\overline{U}^*(\tau)\mathrm{BLU}]\} \tag{3.46}$$

For the "open loop", $\phi(\tau,0)$ is constant so $q_b^*(\tau)$ has a similar variation as $\overline{U}^*(\tau)$. Figure 3.8 indicates how q_b^* varies with time t^* at different BLU. In the computation U_g^* from Problem 1 is used instead of $\overline{U}^*(\tau)$ from Problem 3, in order to save computation time. This is a conservative approach since U_g^* is smaller. It can be observed from Figure 3.8 that q_b^* decreases along with t^*, similar to conductance U^*. When BLU is very small, the q_b^*

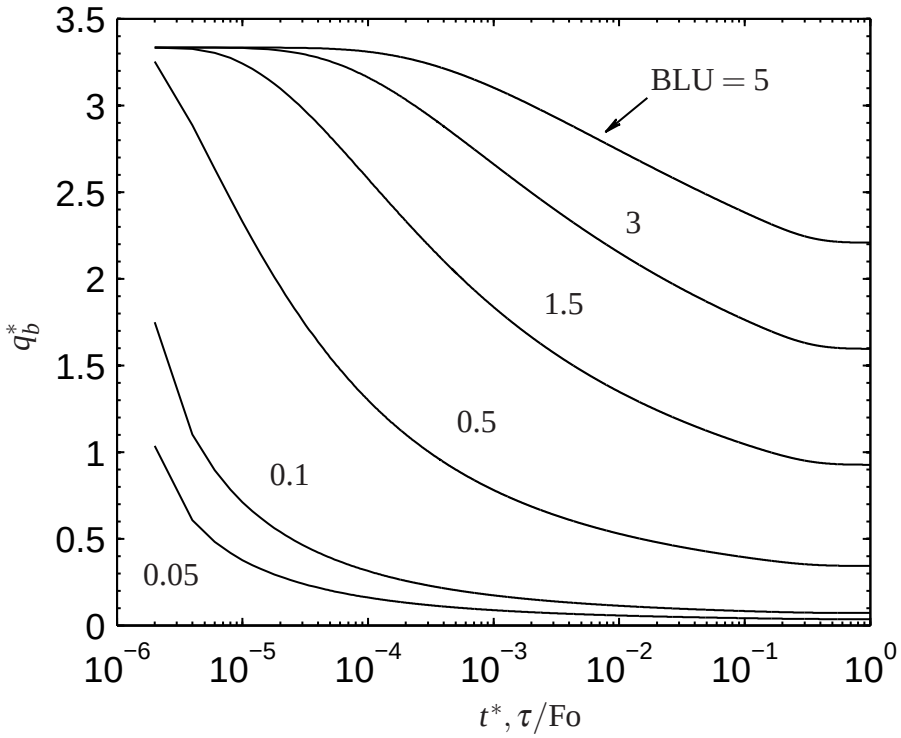

Figure 3.8: Comparison of $q_b^*(t^*)$ with different BLU for Problem 1, with $\varepsilon = 0.3$.

is also very small. When BLU is larger than some value, such as 1, q_b^* will start from $1/\varepsilon$ and then decreases along the t^*. If q_b^* is larger than 1, the heat transfer rate over borehole is larger than that through heat pump. In other words, the borehole is capable of delivering a heat transfer rate larger than the load on the heat pump. There is a critical time however,which is denoted as breakthrough time, t_b^*, when $q_b^* = 1$. The breakthrough time is determined by

$$q_b^*(t_b^*) \equiv 1 = \frac{1}{\varepsilon}\{1 - \exp[-\overline{U}^*(t_b^*)\mathrm{BLU}]\}$$

for Problem 1 since $\phi(\tau, 0) \equiv 1$. At the breakthrough time, t_b^*, the heat transfer rate over the borehole matches that across the heat pump. Figure 3.9 shows how breakthrough time t_b^* varies with BLU. It can be observed from this figure that t_b^* increases as BLU increases,

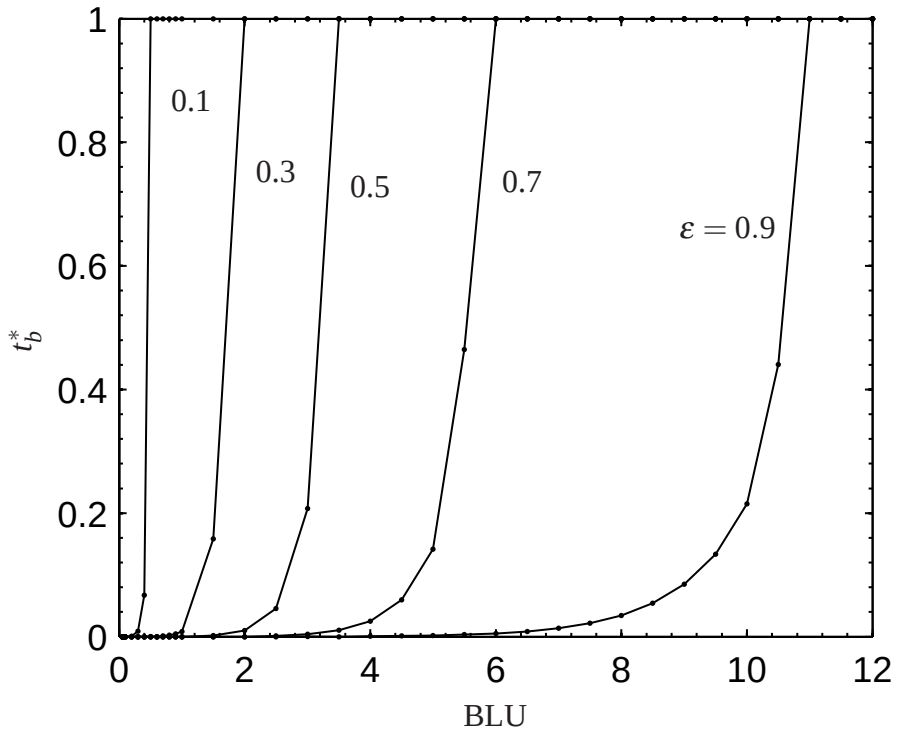

Figure 3.9: Relationship of t_b^* with BLU at different effectiveness ε for Problem 1.

since $\overline{U}^*$ decreases with time. Potentially more useful from a practical standpoint, one could determine the BLU necessary to reach the breakthrough point, $q_b^* = 1$, at the time when the conductance has reached the point of being nominally steady, t_∞^*, as defined in Equation 3.31. Referring to this dimensionless borehole length as BLU_∞, it is defined for Problem 1 by,

$$q_b^*(t_\infty^*) \equiv 1 = \frac{1}{\varepsilon}\{1 - \exp[-\overline{U}^*(t_\infty^*)\mathrm{BLU}_\infty]\}$$

From Problem 1 results, the computed values of BLU_∞ are 0.4, 1.5, 2.5, 4.5 and 8.5 for the effectiveness ε of 0.1, 0.3, 0.5, 0.7 and 0.9, respectively.

Similar results can be achieved if $U^*(t^*)$ from Problem 2 is used. Figure 3.10 shows how breakthrough time t_b^* varies with BLU for different values of Bi when $\varepsilon = 0.5$. It can

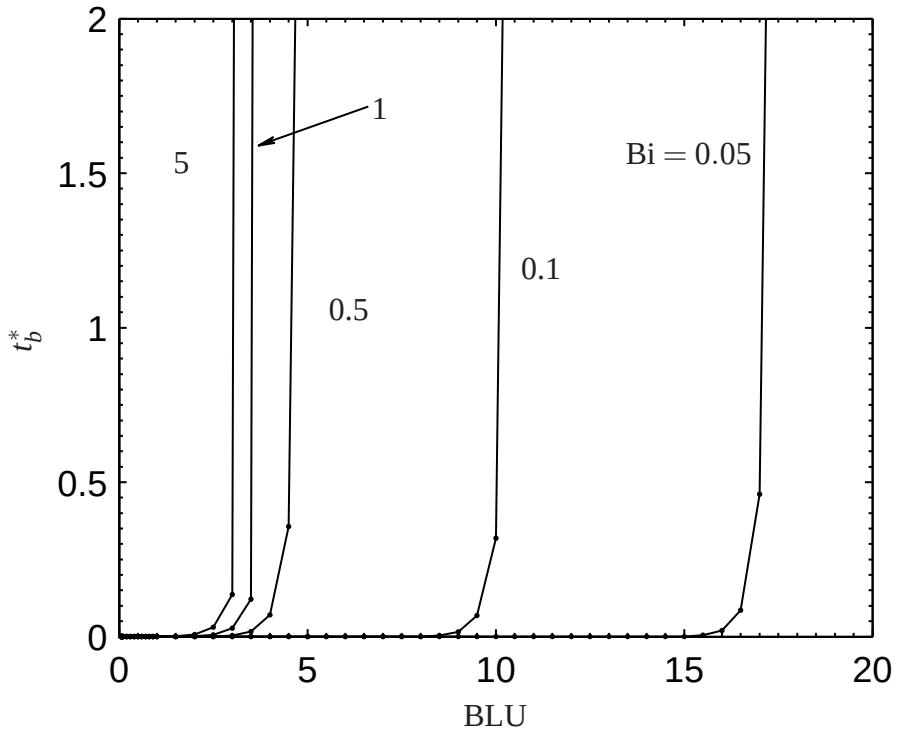

Figure 3.10: Relationship of t_b^* with BLU at different Bi for Problem 2, with $\varepsilon = 0.5$.

be observed from the figure that to produce the same break through time t_b^*, the required BLU decreases when Bi increases. This is because resistance inside borehole decreases when Bi increases, so ground thermal resistance becomes dominant.

Figure 3.11 shows the required BLU_∞ with different Bi and ε. It can be observed from this figure that, when $\text{Bi} = 10$, the required BLU_∞ is 0.4, 1.5, 3.0 and 4.5, respectively when ε is 0.1, 0.3, 0.5 and 0.7. This result is very close to that of Problem 1.

Returning to Problem 3, Figure 3.12 shows how scaled dimensionless conductance $\overline{U}^*(t^*)/U_g^*(t^*)$ varies with t^* at different values of BLU with $\varepsilon = 0.3$. Figure 3.13 shows the results with $\varepsilon = 0.5$, and Figure 3.14 shows the results with $\varepsilon = 0.7$. The $U_g^*(t^*)$ is dimensionless conductance from Problem 1, which does not account for the influence of borehole length and presumes negligible borehole thermal resistance. Thus, only for

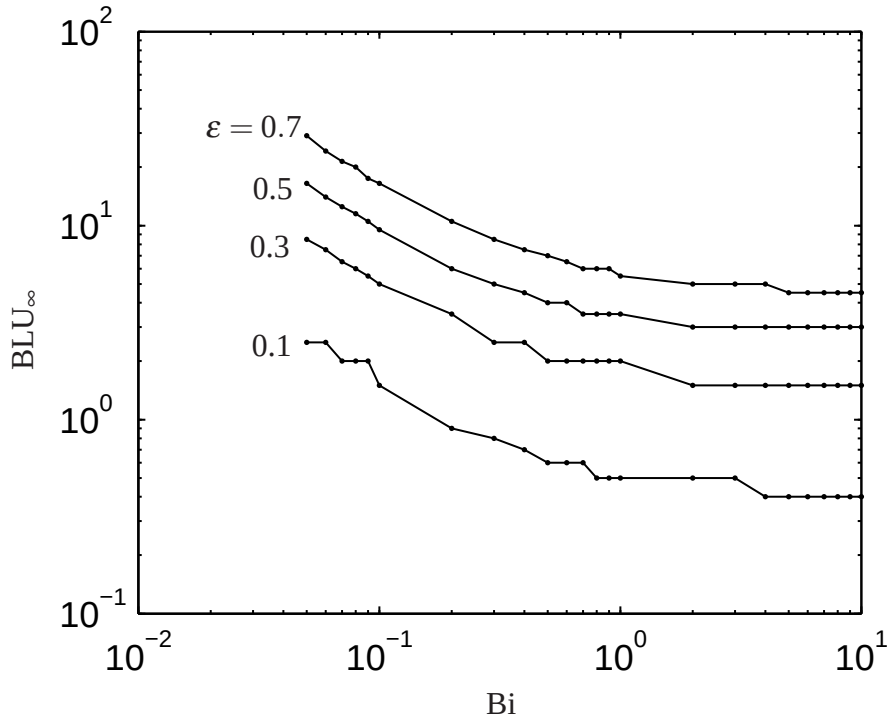

Figure 3.11: Relationship of BLU_∞ with Bi at different effectiveness ε for Problem 2.

the initial period does the length average conductance differ from U_g^*, for BLU $\simeq$ BLU_∞. If the BLU varies from 50% to 150% of BLU_∞, the deviation of scaled dimensionless conductance is reduced to about 10% in 9 hours ($t^* = 10^{-3}$) and reduced to 5% in 4 days ($t^* = 10^{-2}$). The BLU affects the dimensionless conductance U^* primarily in the startup period, for large enough BLU.

To reveal to what extent the BLU affect the U^* in the startup period, the dimensionless transition time t_{tr}^* is computed at different values of BLU, shown as Figure 3.15. In Figure 3.15 the horizontal axis BLU/BLU_∞ evaluates the borehole length and varies from 0.5 to 1.5. The vertical axis provides an indication of, t_{tr}^*, how fast the dimensionless conductance enters the transition period, as described in Problem 1. The figure indicates that no matter the value ε, the bigger the BLU, the longer it takes for the dimensionless

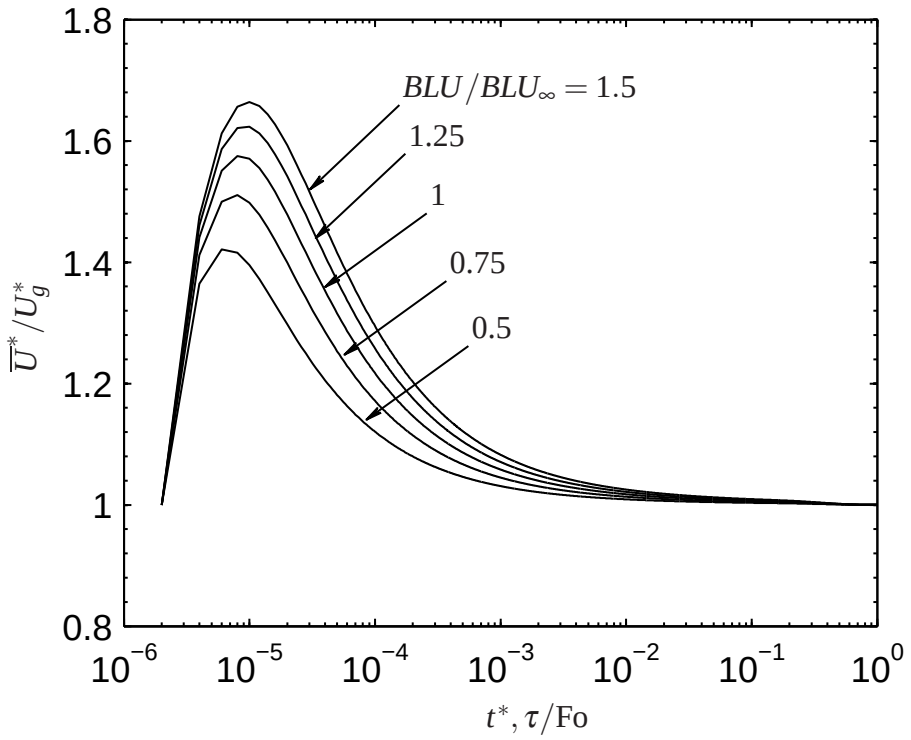

Figure 3.12: History of $\overline{U}^*(t^*)/U_g^*(t^*)$ with different BLU, with $\varepsilon = 0.3$.

conductance to enter the transition period. Inclusion of the borehole length effect increases t_{tr}^*, which is in all cases larger than the t_{tr}^* in Problem 1. In addition, when ε increases, the transition time increases too.

3.5. PROBLEM 4: FINITE FLUID-BOREHOLE THERMAL RESISTANCE, FINITE BOREHOLE LENGTH

This problem can be seen as the combination of Problems 2 and 3. The dimensionless conductance $U^*(t^*, z^*; \mathrm{Fo}, \mathrm{Bi}, \mathrm{BLU})$ therefore has a functional dependence upon depth and time, in addition to its parametric dependence upon Fo, Bi and BLU. Similar to Problem 3, it is assumed that the vertical heat conduction in the ground is negligible; while the boundary condition is different along borehole depth. In that way, this problem can

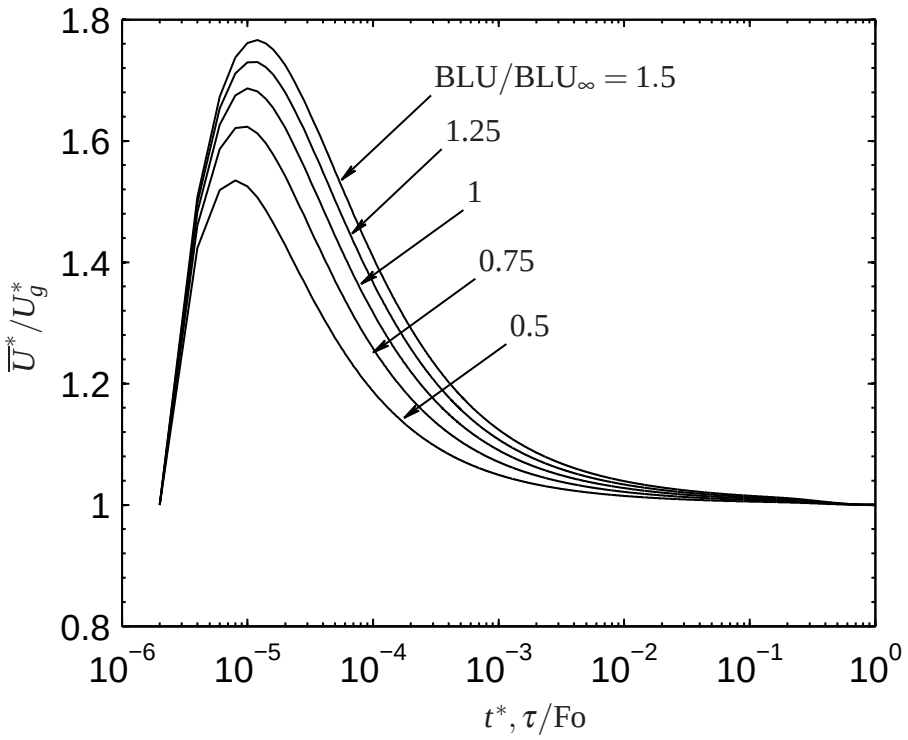

Figure 3.13: History of $\overline{U}^*(t^*)/U_g^*(t^*)$ with different BLU, with $\varepsilon = 0.5$.

be transferred to a series of problems similar to Problem 2, with different borehole surface temperature as boundary conditions.

The Eq. (3.4) still works for this problem, while ground temperature $T(t,z,r)$ depends not only time, but also borehole depth and distance from borehole. Similar to Problem 2, at a particular time t, apply the energy balance from fluid to borehole surface and Fourier's law on the borehole surface, gives

$$\frac{1}{R_b}[T_f(t,z) - T(r,z,r_b)] = -k_g 2\pi r_b \frac{\partial T(t,z,r_b)}{\partial r} \tag{3.47}$$

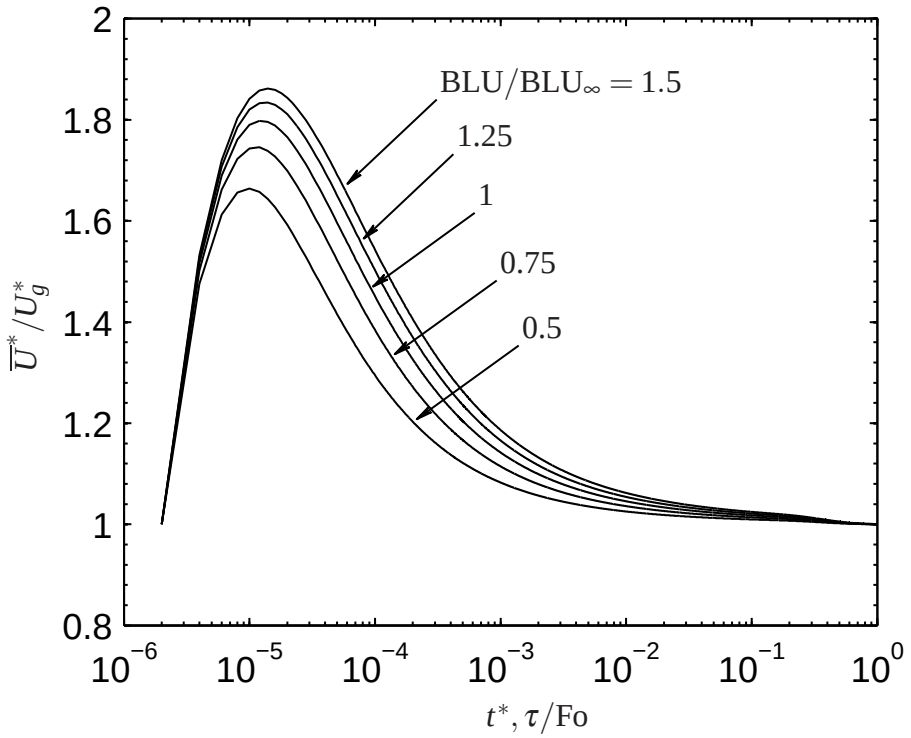

Figure 3.14: History of $\overline{U}^*(t^*)/U_g^*(t^*)$ with different BLU, with $\varepsilon = 0.7$.

Recasting into dimensionless form

$$\frac{1}{\ln r_\infty^*}\frac{\partial\theta(\tau,z^*,0)}{\partial\xi} = -\mathrm{Bi}[\phi(\tau,z^*)-\theta(\tau,z^*,0)] \tag{3.48}$$

This equation is different from Problem 2 only in that ground temperature and fluid temperature also depend on depth. The parabolized one-dimensional diffusion equation, Eq. (3.14), still determines borehole fluid temperature. The initial conditions are the same as Problem 3. In this scheme, the conductance and ground temperature distribution can be solved.

The influence on dimensionless conductance from borehole thermal resistance and borehole length has been addressed in Problem 2 and 4, respectively. To reveal any combined effect of these two parameters together, the histories of dimensionless borehole heat

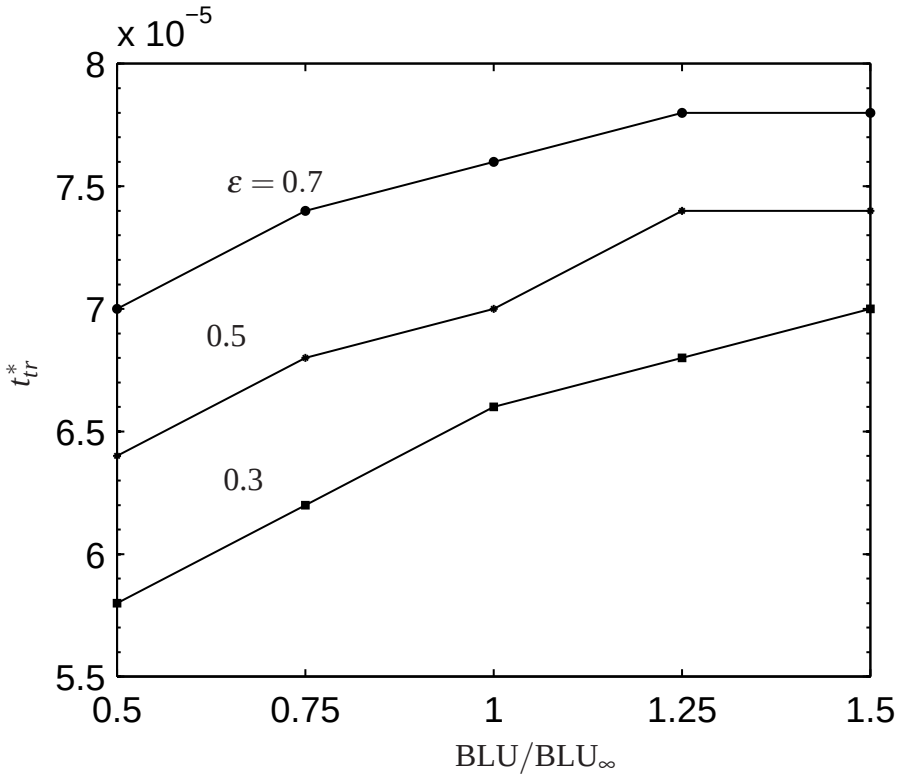

Figure 3.15: Effects of BLU on transition time t^*_{tr} for Problem 3.

transfer rate $q^*_b(t^*)$ of all 4 of the problems are compared in Figure 3.16. In Figure 3.16, the q^*_b is computed with effectiveness $\varepsilon = 0.5$ and $\text{BLU} = \text{BLU}_\infty = 2.5$. The Problem 1 is zero fluid-borehole resistance and infinite borehole length; the Problem 2 is finite fluid-bore resistance and infinite borehole length; the Problem 3 is zero fluid-borehole resistance and finite borehole length; the Problem 4 is finite fluid-bore resistance and finite borehole length. For both Problem 2 and 4, computation is conducted with 3 different values of Bi. According to Figure 3.6, the $\text{Bi} = U^*_{g,\infty}/2$ lies in the range where Bi significantly affects conductance; $\text{Bi} = 2U^*_{g,\infty}$ lies in the range where Bi has moderate influence on conductance; $\text{Bi} = U^*_{g,\infty}$ lies between the two. Several observations can be made from this figure. Firstly, the q^*_b from Problem 3 is very close to that of Problem 1, and that from Problem 2 is nearly the same as that of Problem 4. It can also be inferred that no matter for zero

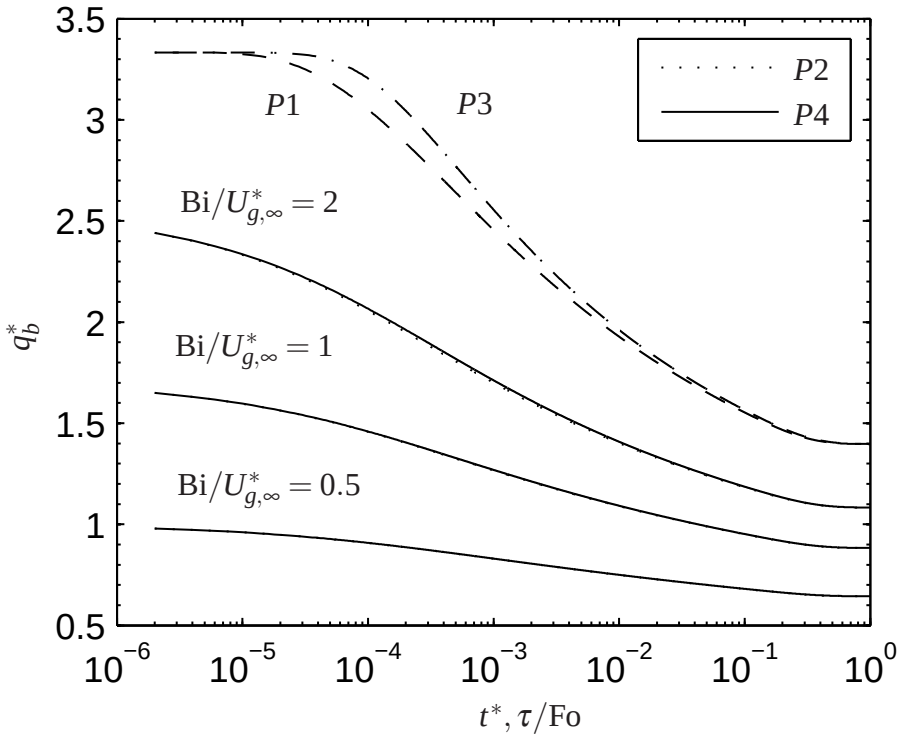

Figure 3.16: Dimensionless heat transfer rate q_b^* from all "open loop" problems, with BLU $= 2.5$ and $\varepsilon = 0.5$. $P1$, $P2$, $P3$ and $P4$ denote the results of Problem 1, 2, 3 and 4. For Problem 2 and 4, 3 different Biot Numbers are considered, they are $\mathrm{Bi}/U^*_{g,\infty} = 2$, $\mathrm{Bi}/U^*_{g,\infty} = 1$ and $\mathrm{Bi}/U^*_{g,\infty} = 0.5$. The results of Problem 2 and Problem 4 are nearly the same with particular Bi.

fluid-borehole resistance or finite fluid-borehole resistance conditions, the borehole length effect on dimensionless conductance is minimal when BLU $=$ BLU$_\infty$. Then the q_b^* from Problem 2 has significant deviation with different values of Bi, even when $t^* = 1$ which represents a whole year period. Finally according to the behavior of q_b^* from Problem 2 and Problem 7, there is no combination effect on dimensionless conductance of BLU and Bi.

3.6. SUMMARY

In this section several “open loop” problems have been introduced which vary in the degree to which they capture key aspects of U^* determination.

The “open loop” which keeps inflow temperature to be constant assumes there is a heat source or heat sink between heat pump and the borehole. Problem 1 provides the simplest non-trivial case of the “open loop” problems. This problem assumes the fluid temperature to be uniform at the borehole entrance, ignores variation of U^* with depth, and neglects fluid-borehole thermal resistance. The numerical results match well with the analytical results provided by Ingersoll. The history of dimensionless conductance $U^*(t^*)$ is divided into three periods: startup period, transition period, and stable period. The division between the startup period and transition period is called t^*_{tr}, and the division between the transition period and stable period is called t^*_∞.

Problem 2 accounts the finite fluid-borehole resistance on the basis of Problem 1. The Bi is used to measure the thermal resistance from fluid to borehole surface. When Bi is very small, the Bi dominates the dimensionless conductance; when Bi is an order of magnitude larger than U^*, identical when $\mathrm{Bi}/U^*_g = \mathscr{O}(10)$, the borehole thermal resistance is irrelevant and results are identical to Problem 1. Figure 3.6 is useful to read the dimensionless conductance without computation.

Problem 3 accounts the finite borehole length on the basis of Problem 1. This problem is converted to a series of Problem 1 with different fluid temperature along the borehole depth. In this way, the two dimension problem is parabolized simplified as a series of one dimension problems, which can save the computation time. The results indicate that the effect of finite borehole length is to enhance the heat transfer compared to Problem 1. The dimensionless conductance $U^*(t^*, z^*)$ increases along the depth and has a parametric dependence on Fo and BLU. For “open loop”, the dimensionless break through time t^*_b is introduced to identify the moment the heat transfer rate over the borehole equals that

across the heat pump. For Problem 1 t_b^* increases as the BLU increases. For Problem 2 to produce the same t_b^*, the required BLU decreases as the Bi increases. BLU_∞ is defined as the minimum BLU which makes the heat transfer rate over the borehole not smaller than that across the heat pump for most of the time. As long as the BLU $=$ BLU_∞, the borehole is able to carry on the building load for most of the time. So BLU_∞ is a very useful index for "open loop" problems. For Problem 3, when BLU varies from 50% to 150% of BLU_∞, the deviation of scaled dimensionless conductance is reduced to about 10% in 9 hours and reduced to 5% in 4 days. This result indicates that the BLU mainly affects the dimensionless conductance in short time period. The dimensionless length of the startup period, t_{tr}^* can be used to quantify the BLU's effect on dimensionless conductance in short time period.

Problem 4 accounts for finite fluid-bore resistance and finite borehole length. It can be concluded from the results of Problem 4 that besides the influence of Bi and BLU, there is no combination effect on heat transfer process when both the values of Bi and BLU are finite.

4. STEADY PERIODIC HEAT LOAD

In the “closed loop”, there is no virtual heat sink or heat source between the heap pump and borehole, and the borehole outflow temperature directly affects the borehole inflow temperature. A schematic of the “closed loop” system is shown as Figure 4.1. The load across the heat pump will be totally imposed on borehole at any time, and thus, symbolically, $q_b^*(t^*) = q^*(t)$.

Over the borehole length, the inflow temperature and outflow temperature must still satisfy Eq. (3.45), the integrated fluid energy balance

$$T_f^*(t^*,1) = T_f^*(z^*,0)\exp[-\overline{U}^*(t^*)\mathrm{BLU}]$$

where $\overline{U}^*(t^*)$ is the length-average dimensionless conductance. The expression indicates that the inflow temperature is dependent on the outflow temperature and the outflow temperature depends, in turn, on the BLU. The expectation is that computation of conductance $U^*(t^*,z^*)$ for this “closed loop” will be very sensitive, and computations show this to be true. In fact, including the borehole length dependency proved to be essential to avoiding numerical instability. Therefore it has been treated only the “closed loop” analogs to the “open loop” Problems 3 and 4.

For every infinitesimally small segment of the borehole, Eq. (3.37) is used to compute the fluid temperature.

$$\frac{\partial\phi(\tau,z^*)}{\partial z^*} = -U^*(\tau,z^*)\phi(\tau,z^*)BLU$$

For the “closed loop”, there are several assumptions to be made. First, the initial ground

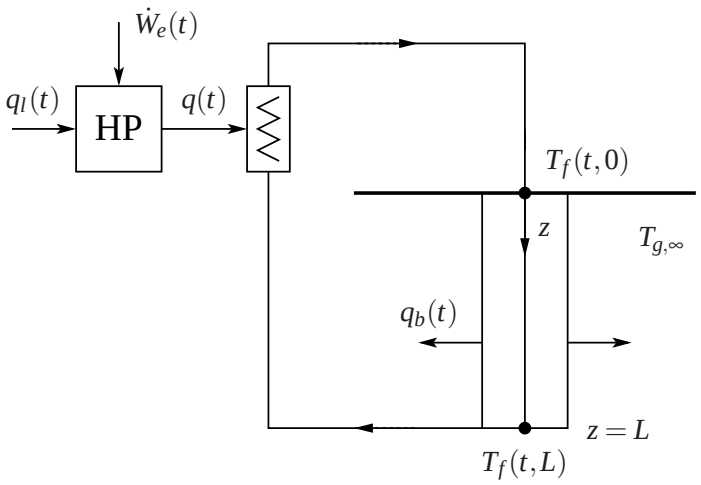

Figure 4.1: The schematic of "closed loop".

temperature distribution is assumed to be uniform, just like in "open loop".

$$\theta(0,z^*,\xi)=0$$

and the initial borehole outflow temperature is assumed to be equal to ground temperature.

$$\phi(0,1)=0 \tag{4.1}$$

Assuming that the load is imposed on the heat pump and borehole when $t^*=0$, a latency of one time step is used for the temperature change across the heat pump. Symbolically, Eq. (3.43) is changed to:

$$T_f^*(t^*+\Delta t^*,0)=T_f^*(t^*,1)+\varepsilon q^*(t^*)$$

and in terms of ϕ,

$$\phi(\tau+\Delta\tau,0)=\phi(\tau,1)+\varepsilon q^*(t^*) \tag{4.2}$$

The diffusion equation for ground temperature is unchanged so that Eq. (3.21), Eq. (3.14), Eq. (3.39), Eq. (4.1), and Eq. (4.2) describe the "closed loop" problem.

4.1. PROBLEM 5: CLOSED LOOP WITH ZERO FLUID-BOREHOLE RESISTANCE, FINITE BOREHOLE LENGTH

This problem is the "closed loop" counterpart of Problem 3, examined as one of the "open loop" problems. As for Problem 3, the fluid-borehole resistance is ignored, so the fluid temperature equals the borehole surface temperature at the same depth, which can be expressed as

$$T_f^*(t^*, z^*) = T^*(t^*, z^*, 1).$$

or in terms of ϕ and θ,

$$\phi(\tau, z^*) = \theta(\tau, z^*, 0). \tag{4.3}$$

As a result, Problem 5 can be summarized by Eq. (3.21), Eq. (3.14), Eq. (3.39), Eq. (4.1), Eq. (4.2), and Eq. (4.3). In addition, the building load is taken to be constant, which means $q(t) = q_{p,m}$ and the dimensionless heat load is $q^*(t^*) = 1$. The ground temperature distribution $T^*(t^*, z^*, \xi)$, fluid temperature distribution $T_f^*(t^*, z^*)$ and the conductance $U^*(t^*, z^*)$ may then be computed.

Figure 4.2 shows results of $U^*(t^*, z^*)$ with $\varepsilon = 0.5$ and BLU $= 2.5$. The selected value of borehole length units, BLU $= 2.5$, corresponds to the value of BLU_∞ for "open loop" with $\varepsilon = 0.5$. For "open loop" problems BLU_∞ was defined as the minimum value of BLU which enables the borehole to satisfy $q_b^* \geq 1$ for $t^* \leq t_\infty^*$. The $U^*(t^*, z^*)$ of "closed loop" provess to behave in a pattern similar to the "open loop". The $U^*(t^*, z^*)$ increases along the depth, so the length average $\overline{U}^*(t^*)$ is larger than $U^*(t^*, 0)$.

The length average $\overline{U}^*(t^*)$ of "open loop" at the same condition is also included in Figure 4.2. The values of $\overline{U}^*(t^*)$ for "open loop" and "closed loop" are essentially the same.

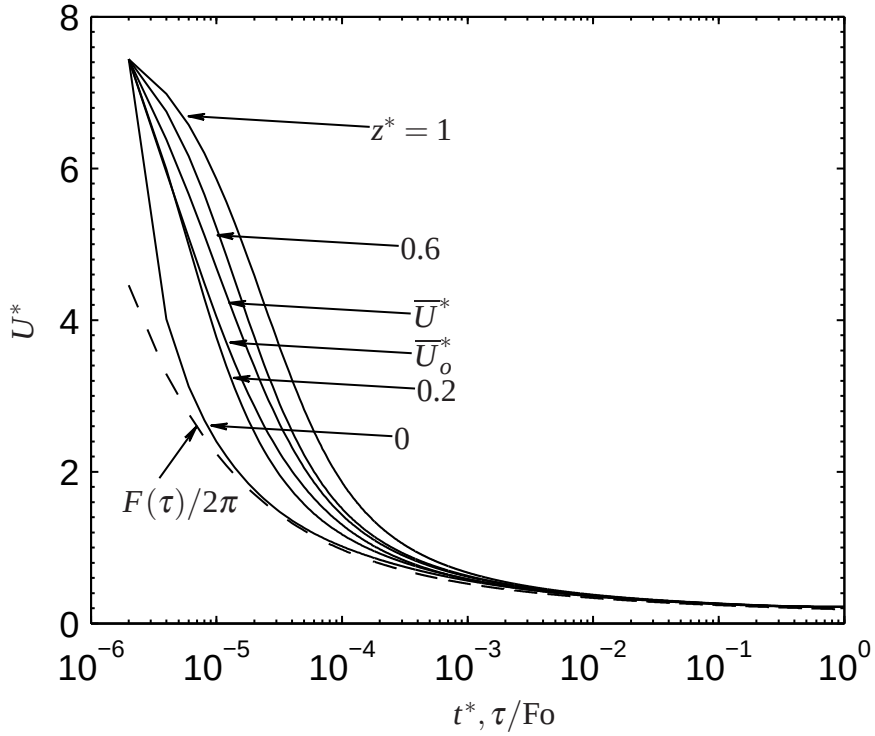

Figure 4.2: The dimensionless conductance along borehole depth for Problem 5, with BLU $= 2.5$ and $\varepsilon = 0.5$. The length average conductance $\overline{U}^*$ is included, as well as the length average conductance of open loop, $\overline{U}_o^*$. The dimensionless positoin $z^* = 0$ denotes ground surface and $z^* = 1$ denotes bottom of borehole.

In the examination of "open loop" conditions, the t_∞^* is introduced to identify the time when the conductance is hardly decreasing and about to settled to a constant value. Since the conductance of "closed loop" is the same as that of "open loop", the t_∞^* is the same for both conditions. In "open loop" conditions, the break-through time, t_b^*, identifies the moment when the heat transfer rate over the borehole equals the load across the heat pump, which means $q_b^* = 1$. However, in "closed loop" operation, the load across the heat pump is imposed on the borehole, which means $q_b^* = q^*$ for all the time. The breakthrough time is therefore meaningless for the "closed loop" condition. However, the "closed loop" condition produces a time-varying outlet temperature. A characteristic which is critically

important to operation of real systems. The fluid temperature history along borehole depth is shown in Figure 4.3. The borehole inflow and outflow temperatures increase simultaneously. The instant dimensionless temperature difference, $T_f^*(t^*,0) - T_f^*(t^*,1)$, is maintained at a constant value of ε as long as building load is constant. This is different from the situation of "open loop". For "open loop" the inflow temperature is constant and the outflow temperature changes following Eq. (3.14), which means that the instant dimensionless temperature difference $T_f^*(t^*,0) - T_f^*(t^*,1)$ varies with time.

For operation of the heat pump system, the borehole outflow temperature is a particularly important parameter. The heat pump may not work effectively if the inlet temperature is too high in cooling season or too low in heating season. To examine how $T_f^*(t^*,1)$ varies with time and borehole length, a series of computation cases have been conducted.

In the "open loop", BLU_∞ was introduced to measure the minimum dimensionless borehole length required to assure the borehole carries the load on the heat pump. This definition won't work for "closed loop", for the load over the borehole is always equal to that on the heat pump. The important quantity becomes the borehole outlet temperature.

Figure 4.4 shows the borehole outflow temperature history at different values of BLU varying from 0.25 to 2 times of BLU_∞, all with $\varepsilon = 0.5$. It can be observed that $T_f^*(t^*,1)$ increases and then reaches a stable value. The larger that BLU is, the smaller the final stable number is. Introducing $t_{f,\infty}^*$ to denote the time when the fluid outlet temperature, $T_f^*(t^*,1)$, reaches a stable condition, associated with Eq. (4.4).

$$\left| \frac{dT_f^*(t^*,1)}{d(t^* F_o)} \right|_{t^*=t_{f,\infty}^*} = 10^{-5} \tag{4.4}$$

The outflow temperature at $t^* = t_{f,\infty}^*$ is defined as $T_{f,\infty}^*$, and referred to as the stable borehole outflow temperature. Applying Eq. (4.4), for $\varepsilon = 0.5$, the $t_{f,\infty}^*$ and $T_{f,\infty}^*$for different values of BLU can be read from Figure 4.4, and the results of $t_{f,\infty}^*$ are plotted as Figure 4.5. It can be seen from Figure 4.5 that when BLU increases, the time required for $T_f^*(t^*,1)$ to become

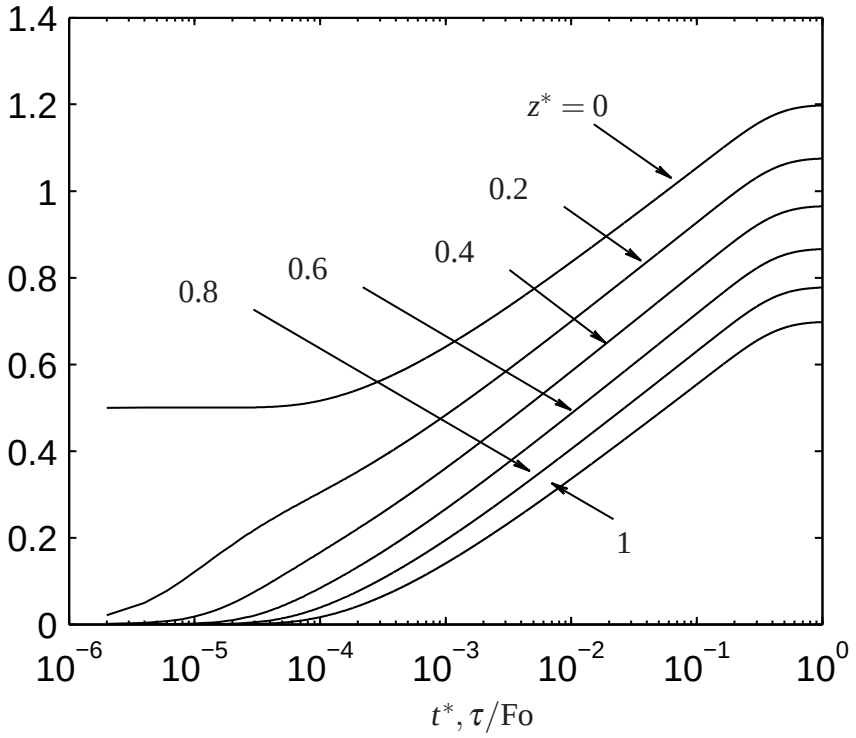

Figure 4.3: History of fluid temperature along the borehole depth, with BLU $= 2.5$ and $\varepsilon = 0.5$.

stable decreases significantly. The stable borehole outflow temperature, $T^*_{f,\infty}$, at different BLU and ε are plotted in Figure 4.6. Because the same borehole length will have different influence on $T^*_f(t^*,1)$ for different values of ε, the ratio $\mathrm{BLU}/\mathrm{BLU}_\infty$ of particular ε is used as the index of borehole length. It can be observed that when $\mathrm{BLU}/\mathrm{BLU}_\infty$ increases, the stable outflow temperature $T^*_{f,\infty}$ decreases significantly, and it can be inferred that if BLU marches to infinite, the $T^*_{f,\infty}$ will be zero. In addition to that, the larger the ε is, the smaller the $T^*_{f,\infty}$ is, because ε measures the potential of heat transfer over the borehole. The high end $\varepsilon = 1$ happens when the outflow temperature is equal to far field temperature ($T^*_{f,\infty} = 0$).

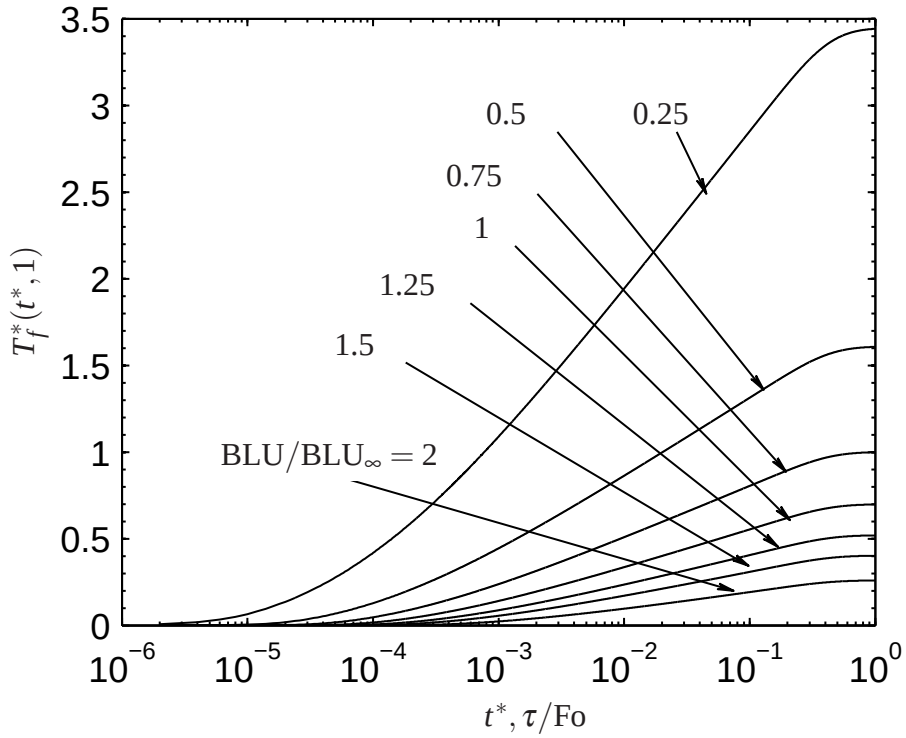

Figure 4.4: The peak outflow temperature with different values of BLU, with $\varepsilon = 0.5$ and $\mathrm{BLU}_\infty = 2.5$.

4.2. PROBLEM 6: CLOSED LOOP WITH FINITE FLUID-BOREHOLE RESISTANCE, FINITE BOREHOLE LENGTH

Similar to the "open loop" Problem 4, the thermal resistance between fluid and borehole surface is now taken to be finite. The only difference between Problem 4 and Problem 6 is that the inflow temperature is constant in the "open loop", while for "closed loop", the inflow temperature is determined at each time step by the imposed heat pump load. Problem 6 may therefore be summarized by Eq. (3.21), Eq. (3.14), Eq. (3.39), Eq. (4.1), Eq. (4.2), and Eq. (3.48). Together, these enable computation of the ground temperature distribution $T^*(t^*,z^*,\xi)$, fluid temperature distribution $T_f^*(t^*,z^*)$ and total dimensionless conductance $U^*(t^*,z^*)$.

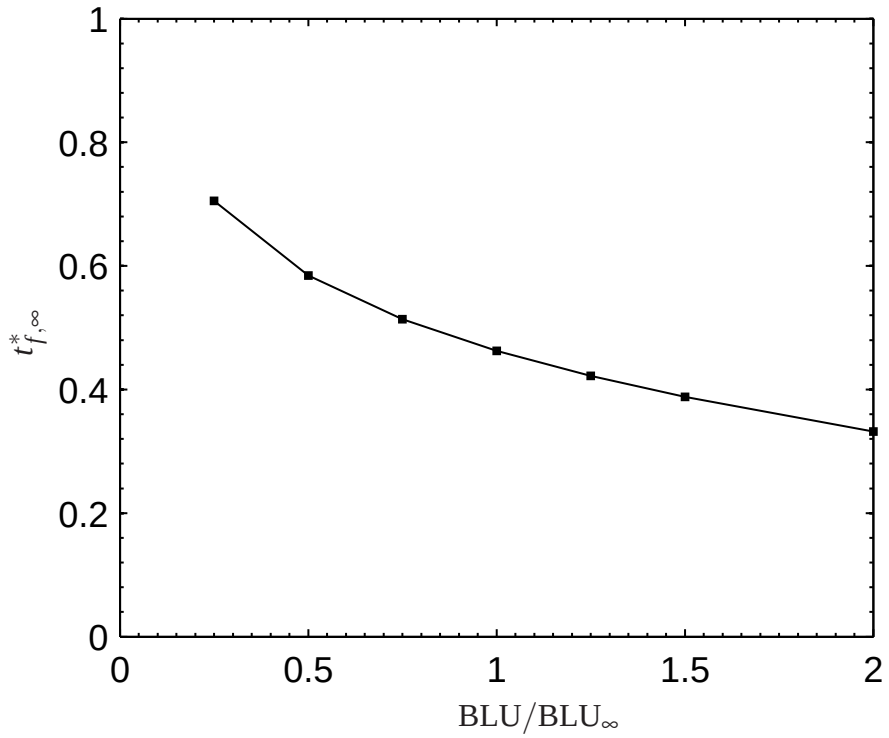

Figure 4.5: The relationship of $t^*_{f,\infty}$ and BLU, with $\varepsilon = 0.5$ and $\mathrm{BLU}_\infty = 2.5$.

The previous "open loop" and "closed loop" problems were limited to constant building load. The reason for this simplification is to separate the influence of building loads on the heat transfer, so the effect of borehole resistance and borehole length can be identified. Relaxing this constraint, it is focused on how the building load affects the heat transfer process. Assume a triangular shaped building load, shown as Figure 4.7. The building load lasts for a dimensionless period of Δt^*_l, which is less than 1. From $t^* = 0$ to $t^* = \Delta t^*_l/2$ the $q^*(t)$ increases linearly from zero to 1 and then decreases to zero after $t^* = \Delta t^*_l/2$.

Figure 4.8 shows the history of dimensionless load $q^*(t^*)$, and borehole inflow and outflow temperature for a case with BLU = 3.125, Bi=10, $\varepsilon = 0.5$ and $\Delta t^*_l = 1$. The results indicate that the shape of fluid temperature variaton in time is similar to the shape of

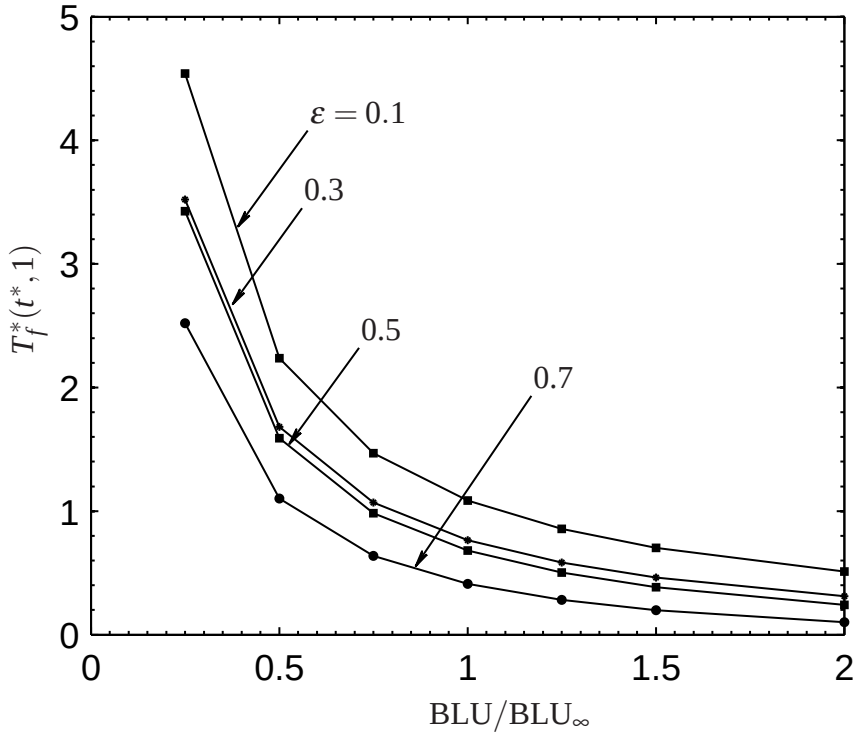

Figure 4.6: The relationship of $T^*_{f,\infty}$ and BLU at different ε. The four curves denotates four different ε, and the BLU$_\infty$ of each ε is different.

load. The fluid temperature increases or decreases following the load, and the highest fluid temperature occurs approximately when the building load reaches its peak value. The larger the load q^* is, the larger the temperature difference between inflow and outflow is. When the load decreases to zero, the inflow and outflow temperature do not drop to zero. For the "triangular" shape load, the maximum value of outflow temperature $T^*_{f,\infty}$ is 0.47. This maximum value is smaller than the maximum outflow temperature of 0.51 observed when the building load is maintained as a constant, $q^* = 1$. The lower energy transfer reduces the maximum observed outlet temperature profile. Figure 4.9 shows the ground temperature history. The temperature history in the ground is similar to that of the fluid in the borehole, and as the radial distance increases, the ground temperature is damped significantly.

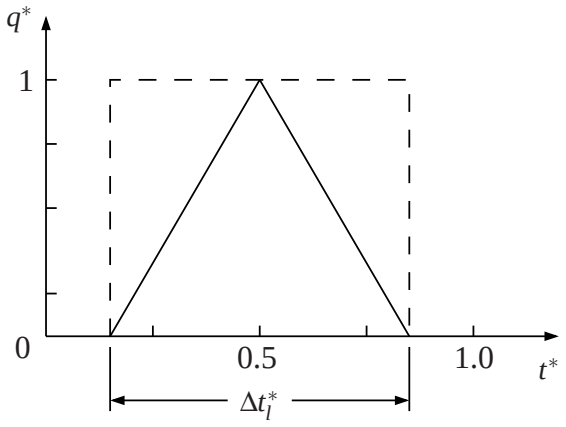

Figure 4.7: Scheme of triangular shaped load.

Figure 4.10 shows the history of dimensionless conductance $U^*(t^*,z^*)$ at different depths as well as the length average value, $\overline{U}^*(t^*)$. The dimensionless conductance behaves in a manner similar to the other problems, except that there are some negative values of conductance when the building load is very low. Heat is therefore being transferred from the ground to the borehole. It occurs because the fluid temperature is nearly in phase with the building load, while the latency effect for the ground temperature is quite significant. There is a period of some time for which the fluid temperature $\phi(t^*,z^*)$ is smaller than the borehole surface temperature $\theta(t^*,z^*,0)$. Because the conductance is dependent on time and depth, to evaluate the influence of building load q^*, the average value of length-average dimensionless conductance, $\overline{U}^*$, over the operation period Δt_l^* can be determined from

$$\langle \overline{U}^* \rangle = \frac{1}{\Delta t_l^*} \int_0^{\Delta t_l^*} \overline{U}^*(t^*) dt^* \tag{4.5}$$

While seemingly straightforward, this method is unstable at the transition period between cooling and heating season, since there may exist some time when the heat transfer direc-

tion between the borehole surface and the ground changes along the borehole depth. This transition results in a vanishingly small temperture difference and a singularity in calculation of $U^*(t^*, z^*)$.

As an alternative, a seasonal equivalent conductance is introduced, which is based on the load and observed temperatures. At a given instant, the building load can be expressed as

$$q(t) = \overline{U}PL(\overline{T}_f - T_{g,\infty}) \tag{4.6}$$

where $\overline{U}$ is the dimensional length-average conductance and $\overline{T}_f$ is the length average fluid temperature. Recalling definitions of dimensionless building load, temperature and conductance, the dimensionless instantaneous heat transfer rate may be rewritten as

$$q^* = (\mathrm{BLU}/\varepsilon)\overline{U}^*\overline{T}_f^* \tag{4.7}$$

A dimensionless, instantaneou length-average conductance may then be computed from

$$\overline{U}^*(t^*) = \frac{\varepsilon}{\mathrm{BLU}}\frac{q^*}{\overline{T}_f^*} \tag{4.8}$$

integrating over the duration of a cooling or heating season,

$$\int_0^{\Delta t_l^*} q^*(t^*) = \frac{\mathrm{BLU}}{\varepsilon}\int_0^{\Delta t_l^*} \overline{U}^*(t^*)\overline{T}_f^*(t^*)dt^* \tag{4.9}$$

a seasonal equivalent conductance $\overline{U}_a^*$ may be defined based upon seasonal-average fluid temperature $\overline{T}_{f,a}^*$:

$$\overline{U}_a^*\overline{T}_{f,a}^* = \frac{1}{\Delta t_l^*}\int_0^{\Delta t_l^*} \overline{U}^*(t^*)\overline{T}_f^*(t^*)dt^* \tag{4.10}$$

Substitute Eq. (4.10) into Eq. (4.9),

$$\overline{U}_a^* = \frac{\mathrm{BLU}}{\varepsilon}\frac{1}{\Delta t_l^*}\frac{1}{\overline{T}_{f,a}^*}\int_0^{\Delta t_l^*} q^*(t^*)dt^* \tag{4.11}$$

where

$$\overline{T}_{f,a}^* = \frac{1}{\Delta t_l^*}\int_0^{\Delta t_l^*} \overline{T}_f^* dt^* \tag{4.12}$$

The seasonal average conductance, $\overline{U}_a^*$, therefore depends on building load q^* and season length Δt_l^* when borehole size is fixed. Figure 4.11 indicates how $\langle \overline{U}^* \rangle$ and $\overline{U}_a^*$ vary with season length Δt_l^*. Both $\langle \overline{U}^* \rangle$ and $\overline{U}_a^*$ decreases as season length increases. The difference between the two results is smaller than 8%, which indicates $\overline{U}_a^*$ is an acceptable equivalent.

Figure 4.12 shows how the peak value of outflow temperature varies with season length Δt_l^*. Clearly, the peak value of outflow temperature increases as the season length Δt_l^* increases. The increase in the energy transferred to the ground drives increased ground temperature and affects the fluid outlet temperature in return.

In many geographic regions, the heat pump system operates in both cooling season and heating season, following an annual cycle. To see how the heat transfer process behaves under an annually periodic building load, the computation is conducted with a triangular shaped building load for five years, with the peak cooling load is equal to the peak heating load. For comparision, the BLU, Bi and ε are kept the same as above, and Δt_l^* is 0.3. Figure 4.13 shows the dimensionless building load. Since the transition period between cooling and heating seasons prevents calculatoin of $\langle \overline{U}^* \rangle$, the seasonal average conductance, $\overline{U}_a^*$, is computed.

Figure 4.14 shows the peak outflow temperature, $T_{f,\infty}^*$, in each cooling season of the five years. It can be observed that the peak outflow temperature in the first cooling season is slightly larger than in the other cooling seasons, and for all five heating seasons, the value of peak outflow temperature is nearly the same. Similar results are produced for

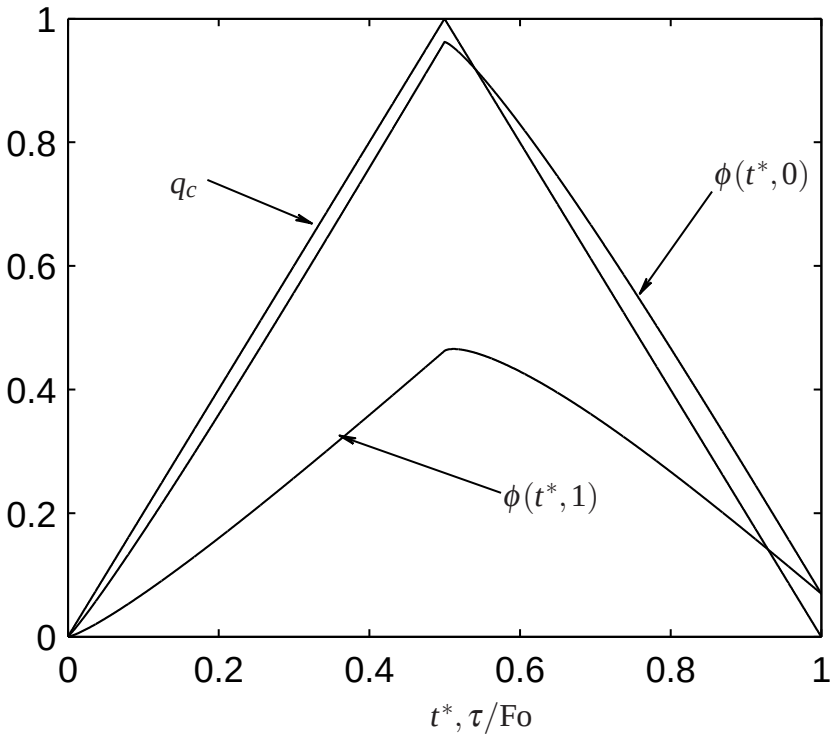

Figure 4.8: History of inflow and outlfow temperature and building load for Problem 6 with the triangular shaped load, with BLU $= 3.125$, $\varepsilon = 0.5$ and Bi $= 10$.

the seasonal average conductance. It can be observed from Figure 4.15 that the seasonal average conductance in the first cooling season is slightly smaller than in the other cooling seasons, and in all the five heating seasons, the values of seasonal average conductance are nearly the same.

4.3. SUMMARY

This section has focused on the "closed loop" condition in which the borehole outflow temperature affects the borehole inflow temperature directly. The heat pump load is imposed on the fluid loop and the borehole inlet temperature reflects the borehole outlet temperature and the load. For "closed loop", two problems have been examined.

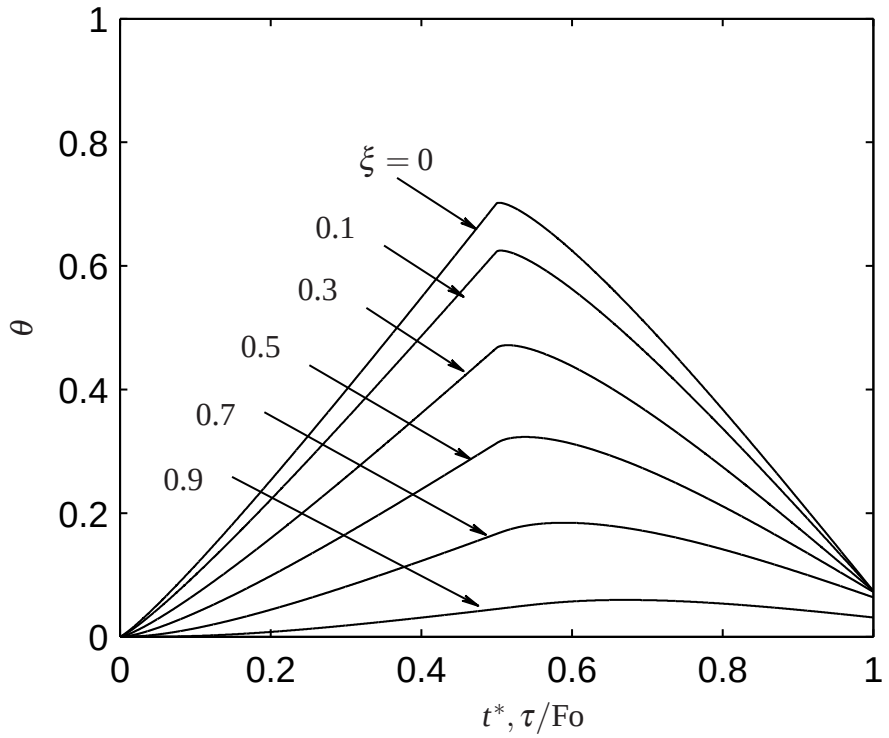

Figure 4.9: History of ground temperature at $z^* = 0.4$ for Problem 6 with triangular shaped load, with BLU $= 3.125$, $\varepsilon = 0.5$ and Bi $= 10$. The radial dimensionless distance $\xi = 0$ denotes borehole surface and $\xi = 1$ denotes far field.

Problem 5 accounts for finite borehole length, with a building load assumed to be constant. The length average dimensionless conductance $\overline{U}^*(t^*)$ of this "closed loop" problem is identical to that of the "open loop". The important concequence of this observation is that the inflow temperature does not affect the conductance. The borehole inflow and outflow temperatures increase simultaneously, and the instantaeous temperature difference $T_f^*(t^*,0) - T_f^*(t^*,1)$ is constant and equal to ε for fixed building load. The outflow temperature increases initially and reaches a stable value, which has been termed the dimensionless peak outflow temperature. The peak outflow temperature is particularly important for design process. The larger the BLU is, the smaller the peak outflow temperature is. The peak outflow temperature of different values of BLU can be read from Figure 4.6. While BLU_∞

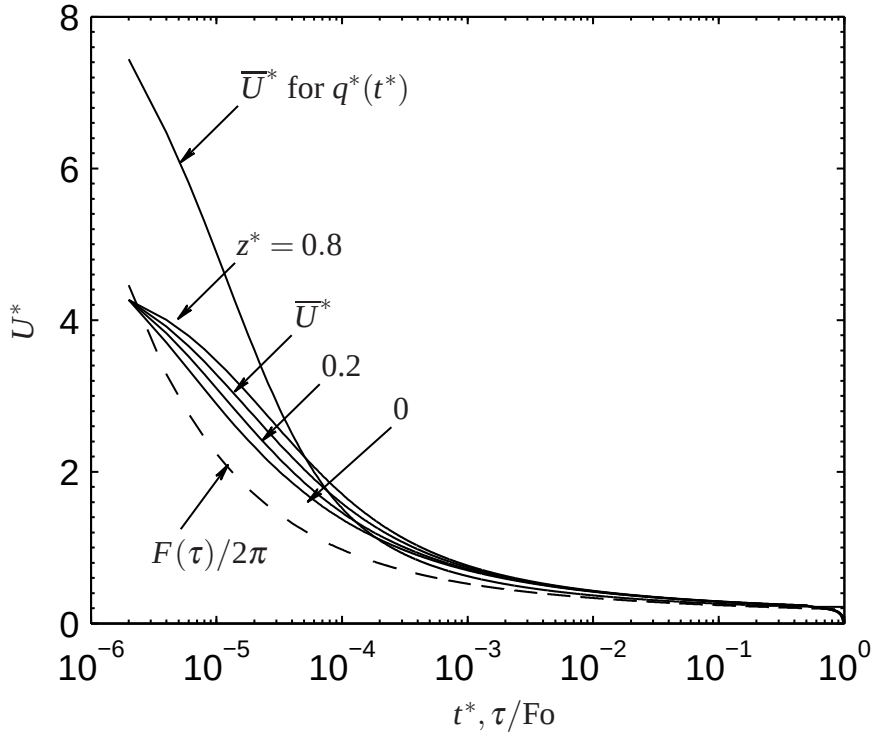

Figure 4.10: Dimensionless conductance along borehole depth for Problem 6, with BLU = 3.125, $\varepsilon = 0.5$ and Bi = 10.

was introduced in the "open loop" problems, and the concept doesn't have a direct consequence in "closed loop", it proves to be the appropriate scale for suitable BLU values even in the "closed loop" problems.

Problem 6 accounts for finite fluid-bore resistance and finite borehole length. These results are the closest approximation to the actual heat transfer process in the borehole of the models developed in this thesis. This problem is mainly used to figure out how the building loads affect the heat process. The triangular shaped load is applied in computation. At first, only a cooling season is considered and the relationship between dimensionless peak outflow temperature and dimensionless season length is plotted in Figure 4.12. The longer the season length is, the larger the peak outflow temperature will be. Another concept defined

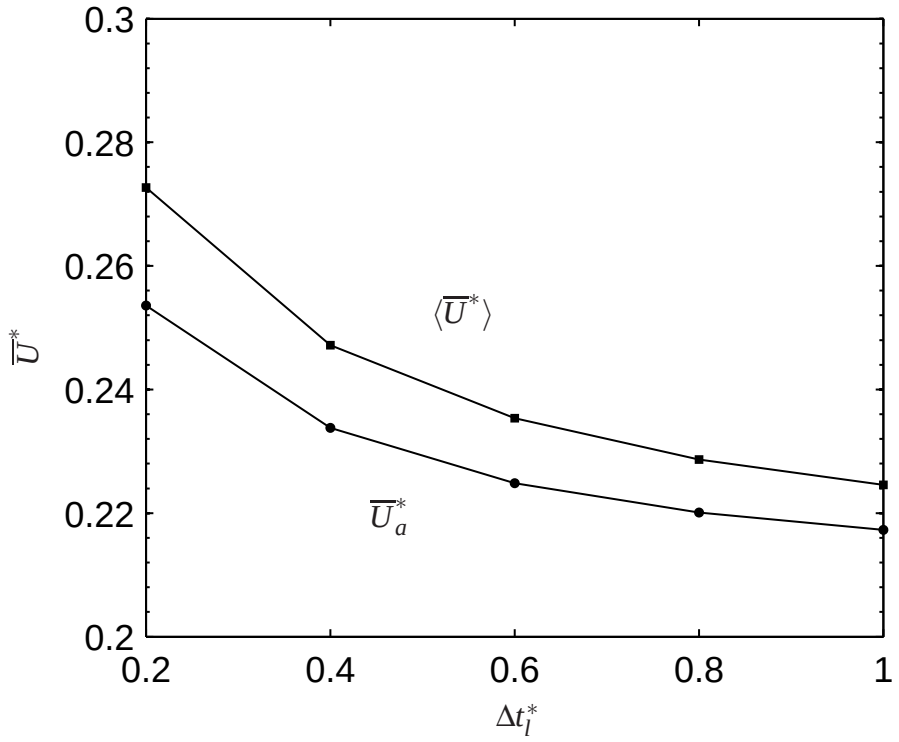

Figure 4.11: Relationship of seasonal equivalent conductance and Δt_l^*, with BLU $= 3.125$, $\varepsilon = 0.5$ and Bi $= 10$. The item $\langle \overline{U}^* \rangle$ is the time average value of length average dimensionless conductance over an operation season; the definition of item $\overline{U}_a^*$ is shown as Eq. (4.11).

to evaluate the building loads effects is seasonal equivalent dimensionless conductance. It is introduced to measure the overall dimensionless conductance through the whole season length. The longer the season length is, the smaller the seasonal equivalent dimensionless conductance will be.

The five-year successive simulation is then conducted. The annually periodic building load contains both cooling loads and heating loads. The peak load value and season length of cooling season and heating season are equal, which makes a balanced load profile. The results of peak outflow temperature and seasonal equivalent conductance of both cooling season and heating season are nearly the same in the five years.

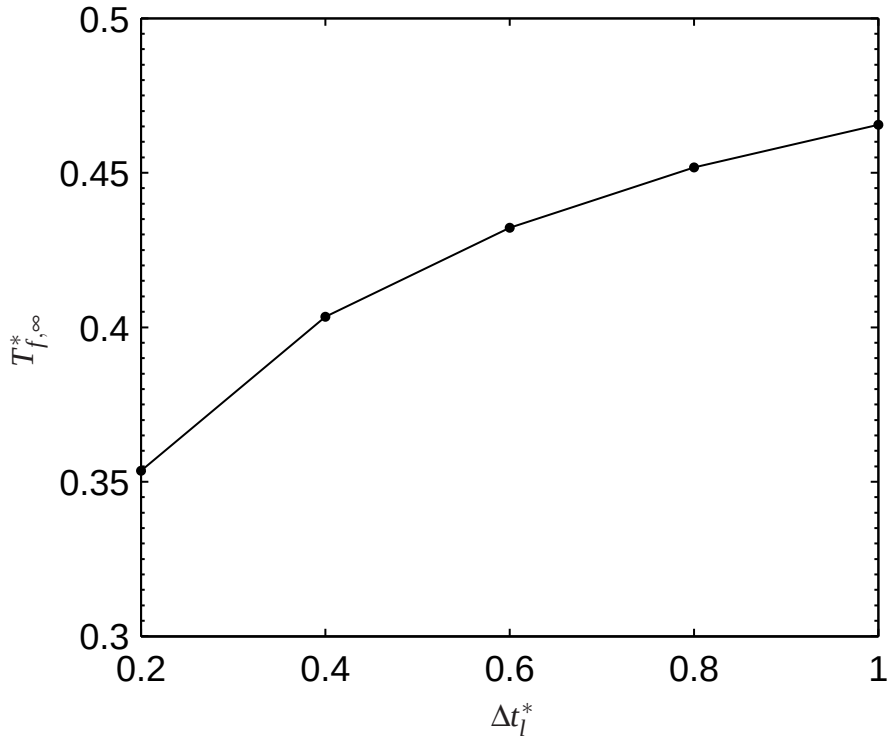

Figure 4.12: Relationship of peak outflow temperature and Δt^*_l, with BLU $= 3.125$, $\varepsilon = 0.5$ and Bi $= 10$.

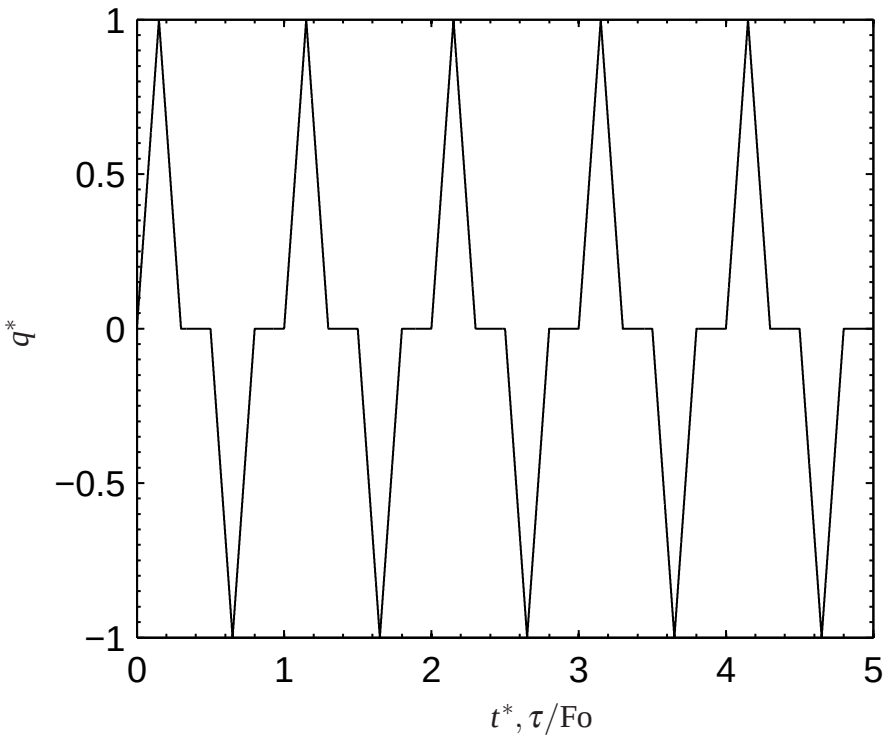

Figure 4.13: History of periodic building load.

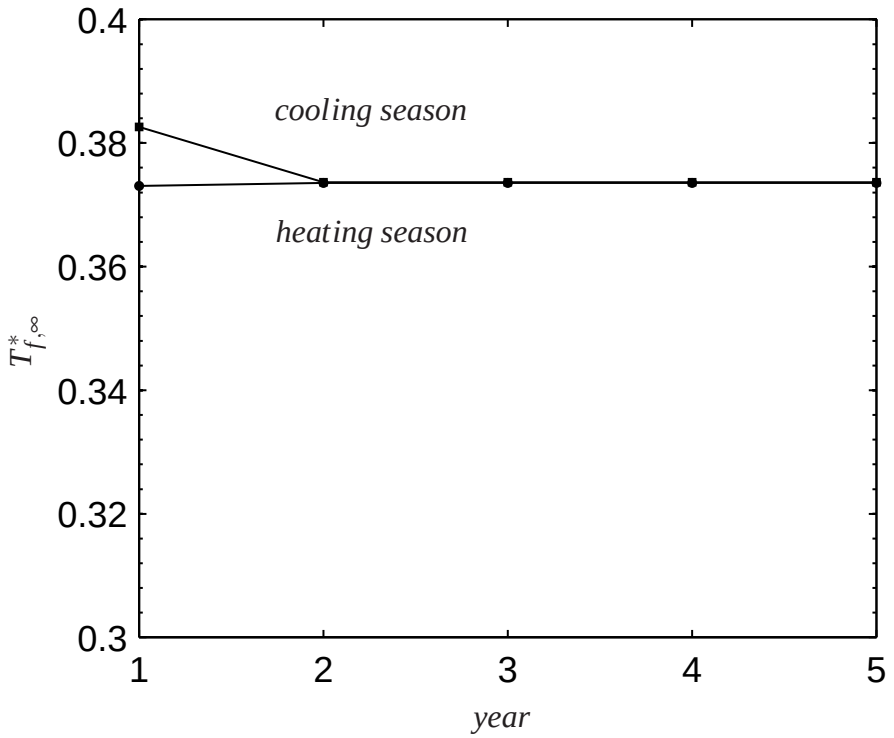

Figure 4.14: Absolute value of peak outflow temperature in each year, with BLU $= 3.125$, $\varepsilon = 0.5$ and Bi $= 10$.

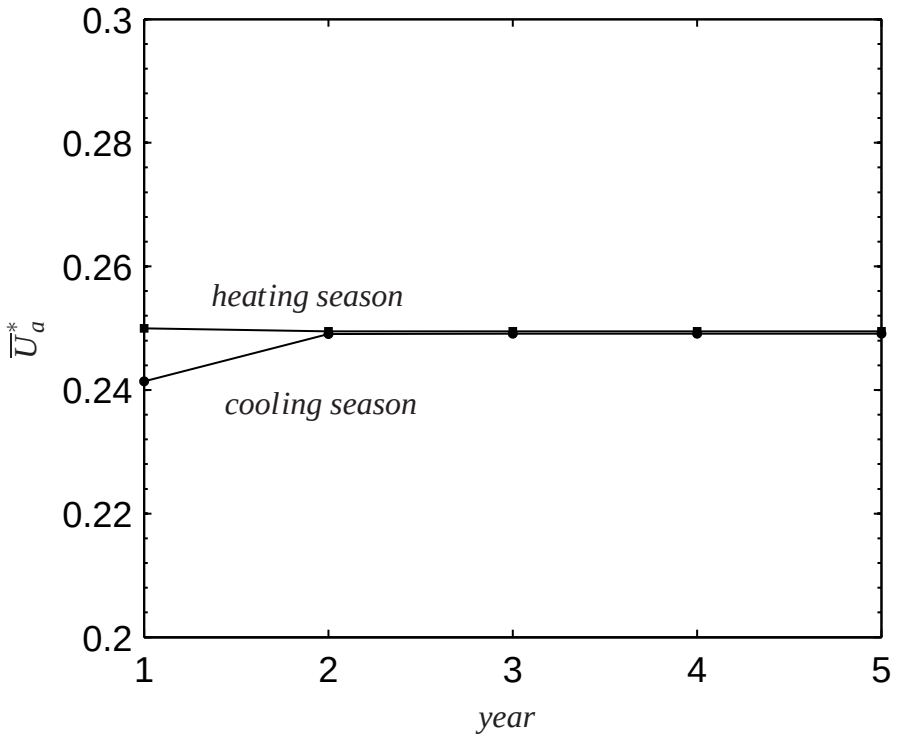

Figure 4.15: Absolute value of seasonal equivalent conductance in each year, with BLU = 3.125, $\varepsilon = 0.5$ and Bi = 10.

5. CONCLUSION

The detailed conclusions are given for each aspect of the work in Sections 3-4. This section provides a brief overall summary of the work and recommendations for future work.

The motivation of this research is to reveal how borehole configuration and building loads affect the borehole heat transfer processes through borehole. The essential insight is the strong parallel to conventional heat exchangers with one fluid of infinite heat capacity. To this end, an effectiveness - BLU framework has been established which proves the ability to estimate required borehole depth based upon specified fluid temperatures and estimated overall conductance. A series of problems are examined to compute, with increasing accuracy, the dimensionless conductance under different assumptions.

The scope of research is divided into two sections: “open loop” and “closed loop”. In “open loop” problems, the inflow temperature is not influenced by the outflow temperature but is specified explicity. In “closed loop”, the inflow temperature is influenced by outflow temperature through specified heat load. The dimensionless conductance is the fundamental outcome for each of the problems. The results show that the time variation of the dimensionless conductance for “open loop” and “closed loop” are essentially the same, the parametric dependencies observed for “open loop” thus apply for “closed loop”.

One of the significant contributions of this work is the introduction and definition of suitable dimensionless parameters. The typical range of these dimensionless parameters are easily calculated with the data provided by ASHRAE handbook. The quantitative results produce insight to the heat transfer process through the borehole, and they can be readily easily applied in a design process, without extra numerical computation. The Biot Number is used to measure the borehole resistance and its quantity relationship to dimensionless conductance is plotted in a form which makes additional computation unnecessary.

The number of borehole length units emerges as a scaled borehole length which, together with dimensionless conductance, dictates performance. The effectiveness ε is defined to measure the potential of heat transfer cross the borehole. The effectiveness ratio determines the scale of the fluid-ground temperature difference.

An important contribution is the use of a parabolized assumption in which the vertical conduction in ground is neglected while the fluid temperature distribution along the depth is accounted for through the boundary condition. In this way, the two-dimensional finite difference system is converted to a series of one-dimensional finite difference system. This scheme provides great economy in computation time.

This research can be viewed as a preliminary step to develop a design method for vertical heat exchangers. For next step, more computation cases can be conducted so that the graphic results on those dimensionless parameters will have higher resolution. And for Problem 6, the unbalanced building loads can be applied. To testify the accuracy of this model, physical building loads can be applied, with the results compared with experimental data.

REFERENCES

ASHRAE. *ASHRAE 2011 Handbook HVAC Applications*, chapter Geothermal Energy, pages 34.1–34.34. ASHRAE, 2011.

M. D. Carli and A. Zarrella. A computational capacity resistance model (carm) for vertical ground-coupled heat exchangers. *Renewable energy*, 35:1537–1550, 2010.

H. S. Carslaw and J. C. Jaeger. *Conduction of Heat in Solids*. Claremore Press., Oxford, U.K., 1947.

P. Eskilson and J. Claesson. Simulation model for thermally interacting heat extraction boreholes. *Numerical Heat Transfer, Part A: Applications: An International Journal of Computation and Methodology*, 13:149–165, 1988.

D. P. Hart and R. Couvillion. *Earth Coupled Heat Transfer*. National water well association, 1986.

Frank P. Incropera. *Introduction to Heat Transfer*. John Wiley and Sons, Inc, 2007.

L. R. Ingersoll. *Heat conduction with engineering, geological, and other applications*. The University of Wisconsin Press, Madison, Wisconsin, 1954.

S. P. Kavanaugh and K. Rafferty. Design of geothermal systems for commercial and institutional buildings. Technical report, ASHRAE, 1997.

H. Su. Fast simulation of a vertical u-tube ground heat exchanger by using a one- dimensional transient numerical model. *Numerical Heat Transfer, Part A: Applications: An International Journal of Computation and Methodology*, 60:328–346, 2011.

Cenk Yavuzturk. *Modeling of Vertical Ground Loop Heat Exchangers for Ground Source Heat Pump Systems*. PhD thesis, Oklahoma State University, 1999.

VITA

Chou Shen graduated in May 2008 with his B.S. degree from the Department of Heating, Ventilating and Air-conditioning Engineering, Southwest Jiaotong University. In June 2011, he received his Master of Science degree from the Department of Heating, Ventilating and Air-conditioning Engineering, Southwest Jiaotong University. From September 2011 to August 2012, he enrolled at Missouri University of Science and Technology as a graduate student in Civil Engineering. In September 2012 he transferred to the Mechanical Engineering at Missouri University of Science and Technology. Chou Shen received his Master of Science degree in May 2014.